



A heat transfer and fluid flow characteristics in a TBHE based on constructal design: An overview

Ahmed Hasan Ahmed¹, Maki H. Zaidan², Manar S.M. Al-Jethelah²

1. Technical Institute, Renewable Energy Research Unit, Hawija, Northern Technical University, Iraq.

2. College of Eng., Department of Mech. Eng., Tikrit University, Tikrit, Iraq.

Article Informations

Received: 29 December 2022

Received in Revised form: 25 January 2023

Accepted: 15 February 2023

Published: 19 February 2023

Corresponding Author:

Ahmed Hasan Ahmed

Email:

ahmedhasan_hwj@ntu.edu.iq

Key words:

Heat transfer, Fluid flow, optimal solutions, optimal design.

ABSTRACT

With the beginning of the industrial revolution in the eighteenth century, ICE, refrigeration equipment, and power stations developed. All of the above devices use TBHE. The recent increase in energy demand is important, which led researchers to find optimal solutions to save the largest amount of energy. The objective of this review can be summarized in the research published in the field of TBHE of all kinds. In order to improve the performance of the TBHE, two basic conditions must be met, the first is to increase the CHTC, and the second is to reduce the PD across the HE. In order to reach this goal, many influential variables must be studied, including pipe diameters and shapes, vertical and horizontal distances, fin shape, and installation method, in addition to the arrangement of the tubes through the TBHE. It was in the form of IL or staggered, the type of flow that was stratified or turbulent. The most important variables affecting the performance of HEs can be summarized in general. The shape of the pipes had a greater urgency in the process, as the flat pipes had better performance than the circular TBHE. The PD and the CHTC are a function of the Reynolds number, as both increases with the increase in the Reynolds number. Therefore, studies in this field must be intensified to obtain the optimal design TBHE, considering all the above variables.



© THIS IS AN OPEN ACCESS ARTICLE UNDER THE CC BY LICENSE: <https://creativecommons.org/licenses/by/4.0/>

1. Introduction

With the beginning of the industrial revolution in the eighteenth century, the manufacture of IC engines, refrigeration devices, and power stations developed. Therefore, it became necessary to search in the field of HEs to release as much heat as possible to cool those devices. Given the wide use of HEs in industrial applications, a lot of research has been done to improve thermal efficiency. Increasing efficiency leads to cost reduction. The research includes selecting working fluids with high specific heat, the type of flow to ensure a high heat transfer coefficient, and the type of metal and shape [1-3]. The paper is organized according to the following, a general review of heat transfer and flow in TBHE Paragraph 1. The effect of speed, pipe diameters, shape, row arrangement, distance, fin shape and installation, and pipe shape were also discussed in Fluid flow parameters and designed TBHE. Optimal tube-to-tube and fin-to-fin spacing with CHTC and minimum PD Paragraph 3,4. Paragraph 5 highlights heat transfer and flow in the HE. The other figure is the flat tube shown in Section 6. Recently, researchers tended to apply the Constructal theory from Adrian Began in the field of TBHE; two types of studies can be classified in this field, single and multiple scales, as shown in Part 7. Section 8 illustrates the missing point of a new study and proposed future work. In the end, paragraph 9 most important conclusions.

2. Background of TBHE

Cross-flow over TBHE is frequently observed in heat transfer equipment such as power plant condensers and evaporators, refrigerators, and air conditioners. In such apparatus, one fluid goes through the tubes while the other moves perpendicularly across the tubes. Flow through the tubes may be studied by taking into account flow through a single tube and multiplying the findings by the number of tubes. See figs. 1 and 2 to see the flow through a collection of tubes and then determine the maximum fluid velocity [4]. This is not the case, however, for flow over the tubes, as the tubes influence the downstream flow pattern and turbulence level, and hence heat transfer

to or from them. Within 30 Re 3000, a two-dimensional numerical study of the transient flow in a round and square tube HE was conducted to determine PD and heat transfer parameters [5]. Comparing the model's theoretical conclusions to previously reported experimental data [6] 2D numerical investigation of steady-state laminar HE in HE of circular tubular banks with low Re number [7,8], numerical and experimental examination of flow in a bundle of oval cylinders [9,10]. Using an FDM, the momentum and Ee have been determined. The findings of the Nu number shown on the tube's surface were documented by [11, 12]. In the design of HEs, the significance of heat transfer and fluid flow through tube banks is well-known. Extensive experimental [13-17] and numerical investigations [6,18-21], both experimental and numerical [22-25], have previously been conducted on circular tube banks. The numerical study of laminar forced convection in a two-dimensional steady state in a circular cylinder bank with square and non-square-line configurations. The investigation reveals that the first tube has the maximum heat transmission rate compared to the other. In addition, the PD increases dramatically when the transverse pitch to diameter ratio decreases [26]. Experiments were done to examine the heat transfer in the plate-fin HE at laminar flow within the range of 30 to 3000 Re. The study revealed that the average heat transfer coefficient rises by 15%-27% and the PD increases by 20%-25% compared to In direct order [27]. Perform an experiment to demonstrate the air/water cross-flow finned tube HE's performance characteristics. The HE has been tested in the range of Re numbers between 400 and 1500, depending on the hydraulic diameter as a characteristic. The mass transfer coefficients and convection were determined from the Colburn j factor and FF against Re number. Due to the presence of a film temperature, [28] it is also regarded to be a somewhat improved heat transmission medium. Based on previous studies published in the literature, one can conclude that tube shape and arrangement greatly influence heat transfer [29]. Experimentally, [30] investigated the influence of airflow rates and average particle sizes on thermal fluid characteristics in tube banks for both cascading and gradient configurations of gas-particle flow. Another impact of geometric characteristics such tube pitch, fin spacing, and tube diameter on COP

and the ratio of heat transfer rate to power dissipation PD ($Q/\Delta P$). The optimal value of $Q/\Delta P$ was determined through numerical simulation [31]. [32] provides a stable mathematical model for hybrid arrangements of circular and elliptical tubes with fins. The temperature distribution and fin efficiency of the first and second rows of elliptical finned-tubes HEs were determined numerically using the CHTC collected experimentally via the sublimation of naphthalene technology and a portion of similarities with the transfer of heat and mass [33–36]. The finite volume method for computing conjugate heat transfer and flow characteristics in three dimensions in flat plate finned-tube HE is investigated. All of the flow patterns, pressure distribution, heat flux distribution, heat transfer coefficient distribution, and fin efficiency were depicted with a fixed shape in relation to the Re number. They discovered that the downstream fin is significantly less effective than the upstream fin. In addition, they asserted that the limited conductivity of the tube's wake caused the reversal of heat transmission [37]. The steady-state laminar incompressible flow over a tube bundle has been developed and used to solve the two- or three-dimensional energy equation and NSE [38–41]. The use of numerical simulations or models to predict the fluid flow and heat transfer in tube banks has made tremendous efforts for development. They have been applied in many previous studies at an in-line configuration only [42–54], to an SG only [55–66], and both configurations [67–71]. Numerous researches have been conducted in the field of heat transfer and fluid flow in the analysis of two- and three-dimensional HEs with fins and without fins using FLUENT [72–86], ANSYS CFX [87–91], CFX4.4 [92], COMSOL Multiphysics [93]. A small number of scholars have presented numerical analyses of three-dimensional modeling for finned-tube HEs. [94] examines a fully developed flow with periodic boundary conditions to model fluid flow and heat transfer using tubes placed in an in-line configuration. [95] conducted a computational and experimental analysis of the effect of fin spacing on the hydrodynamics and heat transfer for fluid flow through a three-dimensional finned tube with a single row configuration in the range $60 < Re < 1460$. Similar research is examined in [96]. This approach is acceptable for getting the quantitative coefficient of heat transfer for the plate fin [97] when the measured

coefficient of heat transfer is $Bi < 0.058$. Different applications were suggested, like enhanced heat transfer in HE [98].

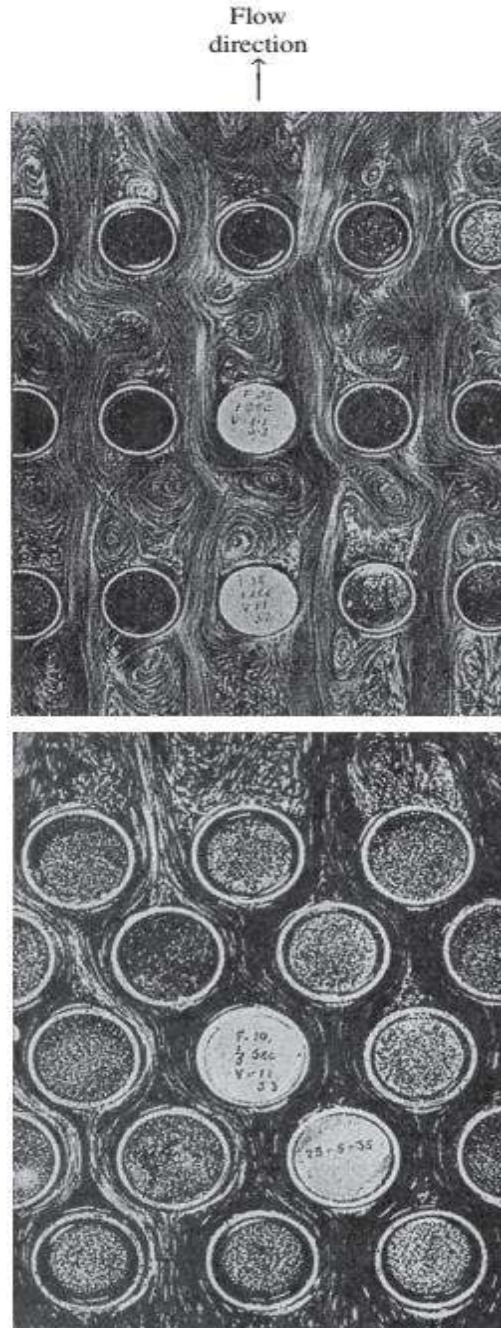


Figure 1: Flow patterns for staggered and IL TBHE.

The fluid flow in TBHE carried out using PIV an SG with $4.8 \times 10^3 \leq Re \leq 14.4 \times 10^3$ [99], at $Re = 9300$ [86],

with $237 \leq Re \leq 55.9 \times 10^3$ [100], and at $Re = 2250$ [101], both in-line/SGs with $5.4 \times 10^3 \leq Re \leq 29.7 \times 10^3$ [102]. A comprehensive study was conducted to review research in the field of exchangers to show the effect of many variables on the performance of HEs, mainly the pressure difference and heat transfer [103].

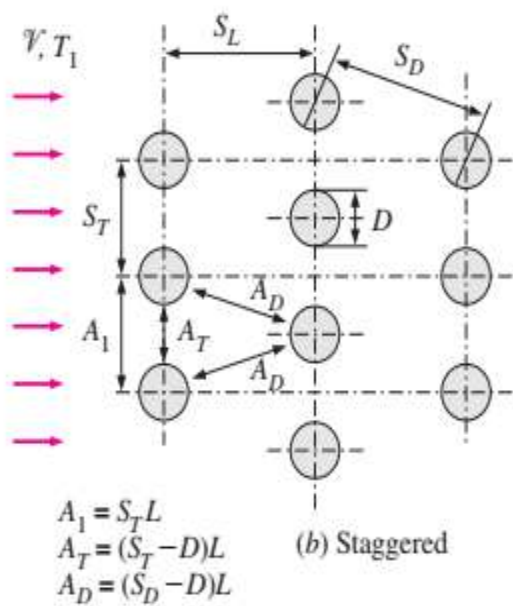
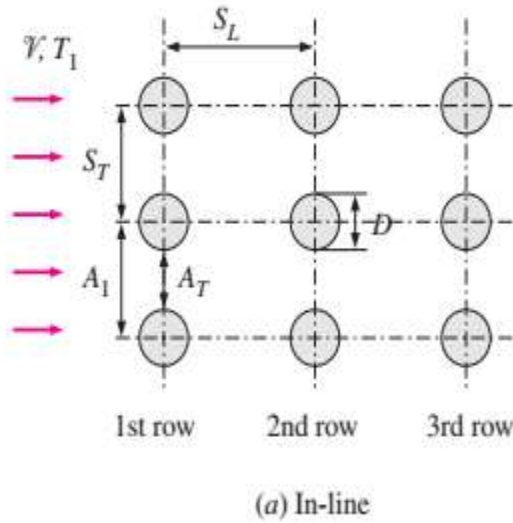


Figure 2: Arrangement of the tubes in IL and staggered TBHE (A₁, A_T, and A_D are flow areas, and L is the length).

3. Fluid flow parameters and designed TBHE

The design of TBHE, flow conditions, and the installation of longitudinal or transverse fins significantly impact the distribution of the CHTC, the pressure gradient through the HE, and the cost, weight, and required geometry. Combining all the variables above to reach the optimal design is not easy, so studies in this field are intensified. Researchers resort to separating heat transfer and fluid mechanics when necessary, so the separator is the Reynolds number. The general effect of the flow and geometric parameters on TBHE are presented in Table 1. These parameters' more detailed impacts will be shown as follows [3].

3.1 The effect of the superficial velocity

The main shape of the adjacent layer depends on the velocity; it can be said that the adjacent layer is inversely proportional to the velocity. Therefore, we notice areas where the adjacent layer is close to the wall and does not exist in the middle, directly affecting the convection heat transfer coefficient. Therefore, it is necessary to address the selection of the Reynolds number at the characteristic dimension of the irregular or finned shapes. The researchers used the entrance velocity, the average velocity, and the velocity in the smallest area as the reference velocity. The reference velocity is usually defined as the last velocity according to the available literature [104,105]. The study has been done for fluid flow over the ILTBHE by using the finite element technique to estimate the effect of PD on heat transfer. They found that the separation angle from the front point of stagnation decreases with an increase in flow velocity [106]. The convective motion in both ILTBHE and STBHE is solved numerically by the FEM. The transverse and longitudinal pitches fixed at 2 with $40 \leq Re \leq 800$ were studied. The result shows that CHTC is a function of Re [107]. The HE and PD in an ILTBHE were investigated experimentally for Re numbers between $5 \times 10^4 \leq Re \leq 6 \times 10^6$, $0 \leq k/d \leq 0.009$. The results show that the CHTC is a function of Re for all cases, and the maximum enhancement at $k/d = 0.003$ [108].

The Experimental and numerical study of heat transfer and fluid flow in STBHE uses the SIMPLER method to analyze the 3-D of the flow field. The free

stream velocity ranges are 2 m/s–7 m/s. Comparing the experimental data with numerical results showed a good agreement [109]. The temperature distribution in TBHE and the mean CHTC is around 14%–32% in SG compared with [110]. The total thermal resistance value on the waterside is less than 10% at the Re number varied between $1200 \leq Re \leq 6000$. The results indicate that the thermal resistance of air–the side equals almost waterside at $500 \leq Re \leq 1200$ [111]. Numerical studies evaluated frontal air velocity's effect in STBHE at 0.646 m/s to 4.64 m/s [112]. Also, the impact of the inlet air velocity on the Nu number and friction coefficient ranging between 0.4 m/s to 4 m/s by [113]. A numerical and experimental study of FCHT in the air–side STBHE. AT $1082 \leq Re \leq 1649$. The number of relative errors between the numerical and experimental results is around six percent. The deviation between these experimental results and previous work ranges from 7% to 32.4% [114]. The characteristics of airside HT and PD in the experimental work have been done in [115].

3.2 The effect of tube diameter

A numerical studies of heat transfer on the two-pass automobile radiator with oval shape tubes have two diameters, the minor of 6.35-mm and major of 11.82-mm, was investigated. The results showed wakes in the front/behind tube at the second row that lead to the minimization of the heat transfer rate to the lowest value [116,117]. The flow and thermal characteristics of circular and oval tubes were carried out experimentally [118]. The thermal–hydraulic oval tube performance is better than circular tubes [119–121]. The influence of tube diameter on the Nu number and friction coefficient varies from 5-mm to 15-mm at $1000 \leq Re \leq 6000$. Both heat transfer and friction coefficients increase with the tube diameter [113].

The influences of minor–to–major axis ratios are $0.25 \leq Ar \leq 1$, and $5.6 \times 10^3 \leq Re \leq 4 \times 10^4$ in the STBHE. The better thermal performance was eligible with smaller values of Re number and Ar [122]. Unsteady–RANS to simulate HT and PD in TBHE. The study shows that the rise of thermal hydraulic performance is higher than 80%, with a reduction in the tube ellipticity compared with circular tubes [123].

3.3 The effect of tube rows

The arrangement of the rows in the HE attracted the attention of many researchers for several reasons, including the pressure gradient across the tube bundles, the variation of the CHTC from one tube to another, and the type of application. We may need a number of rows exceeding four rows, especially in the zigzag arrangement, to ensure that the fluid passes through the tubes similarly. The impact of the number of rows on the CHTC for an in–line is higher than that of staggered at $N_R \geq 2$ [104,124,125]. Note that the CHTC has become fixed following the 3rd row. Rabas and Taborek, The correction factor of rows, decrease with an increase of rows number at the upper density of fins is 0.984 fins per meter while increased with a small fin density of 0.393 fins per meter [126]. The effect of tube rows on the CHTC for TBHE is also theoretical and experimentally studied [127]. The maximum efficiency at the two rows tube compared with single rows for $200 \leq Re \leq 700$ [128]. The experimental investigation of fluid flow and heat transfer characteristics of TBHE is studied. The results were displayed in $300 \leq Re \leq 20000$, the increases in ΔP with increased tube row numbers for the same frontal air velocity[129]. An experimental study to determine the effect of the tube row number on PD in TBHE. The tube rows various between 2 to 4 for the air velocity changing from $0.9 \text{ m/s} \leq V \leq 4 \text{ m/s}$. The key result from this study is that the increase in the tube rows leads to a decrease in the Colburn and FFs [130]. The effect of tube rows and airflow rate on the j –factor for TBHE for both in–line/SGs were tested experimentally [131]. The results show that the staggered fin and tube configurations enhance the performance of CHTC by seven and ten percent, respectively. The investigate of CHTC from TBHE under an isothermal B.C. The control volume was selected from the fourth row of a tube as a typical cell to study the heat transfer from an in–line or SGs so analytical studies [132]. C-F over TBHE is commonly encountered in practice in heat transfer equipment. The \overline{Nu} number increases by 30%,65% on the 2nd and 3rd tubes, compared with the first tube [133].

3.4 The effect of tube pitch

Early review of the CHTC and PD in the finned or non-finned TBHE with circular tube experimental literature [124,134]. Establishing the relationship between the CHTC and PD depends on air velocity and tube spacing [135]. For the STBHE, the CHTC is bigger for the nearer transverse pitch [135,136]. It would appear that the air velocity will become highest at decreasing the transverse pitch, and this impact will lead to bigger PD and CHTC [137-139]. A two-dimensional analysis was presented for inclined laminar-flow heat transfer in TBHE. The several cases with the inclined flow in the range of $0 \leq \theta \leq 90^\circ$, $1.25 \leq p/d \leq 2.0$, $5 \leq Re \leq 200$, and $1 \leq Pr \leq 528$ [140]. The FEM solves the Ee of heat transfer and fluid flow over inline/staggered TBHE [141-142]. [143] studied the effect of p/d ratios and Re number on average Nu number and PD for $4 \leq Re \leq 40$. An FVM and displayed results for two pitch-to-diameter ratios are 1.5 and 2.0 based on $54 \leq Re \leq 120$ at $Pr=0.7$ [144-146]. A numerical investigated of the HT and PD in TBHE. The pitch-to-tube diameter ratio various from 1.25 to 2.0, $100 \leq Re \leq 1000$, and $1 \leq Pr \leq 100$ for CHF and CST. The forms of the results showed by FF, PD, and CHTC [147]. The following year extended the previous study for heat transfer and fully developed laminar flow over tube bundle HEs For the in-line configuration [148] and both in-line and SGs of the tube [149]. The PD in a round and elliptical TBHE with $200 \leq Re \leq 900$. The results found a reduction in pressure loss of around tubes 30% [150].

The laminar air flow convection heat transfer in the staggered circular TBHE was studied numerically [151]. The results, particularly at lower Re numbers, predict tube bank heat transfers. Employed a naphthalene sublimation technique to calculate CHTC of plain finned and TBHE. The decrease in the tube's pitch leads to more increase in the CHTC while increasing the PD [152]. The hydrodynamics characteristics for the in-line circular TBHE were carried out numerically [153]. The ratios of p/d are 1.45, 1.50, 1.75, 1.85, and 2.00, with $Re \leq 200$. The results showed that the local Sh and \bar{Sh} numbers. Their acquired correlation for \bar{Sh} a number shows good agreement with previous experimental correlations. The influence of tube pitch on CHTC in the circular TBHE for both in-line/SGs was studied analytically [154]. The main results from this study are that the \bar{Nu} TBHE depends on the transverse and longitudinal pitches and Re . The effect of longitudinal and transverse pitches on the CHTC and PD at the staggered TBHE was carried out in three dimensions [155]. The decrease in the transverse pitch causes the increased inlet velocity, enhancing CHTC. The numerical investigations of local CHTC

for the TBHE issue for a wide range of TP, LP, and Re numbers [156-161]. For Pr number [39,51,107,109], and experimental [162]. The numerical 2-D FCHT of airflow over a staggered circular TBHE used the BFC and the FDM. Three transverse pitches of 1.25, 1.5, and 2.0 with $25 \leq Re \leq 250$ were examined. The results showed a higher Nu in the first tube [163]. Ramana et al. [164] An experimental test to influence tube-to-tube distance on the performance of the thermal fluid for both an in-line/staggered TBHE at $200 \leq Re \leq 1500$. Re number enhancement, the CHTC is 100% at the staggered TBHE, whereas the PD in an in-line TBHE decreases around 18%. Experimental and numerical studied for the PD and forced heat transfer over four elliptic tubes in CF with SBTHE for $4000 \leq Re_b \leq 45570$. The transverse, P_T/b , and longitudinal, P_L/b spacing ratios both change between 1.5 to 4.0. the average CHTC has larger values for the four tubes staggered TBHE [165].

In a recent study, the use wall-resolved LES with URANS to investigate the flow over periodic in-line TBHE have carried out. They studied the impact of tube spacing on fluid flow with the three values of the pitch-to-diameter ratio, P/D , 1.4, 1.6, and 2.0, being tested. The results showed that the decreases in P/D led to an increase in the flow deviation [166]. The effect of Re number on the PD and CHTC in a high-performance of an in-line and staggered TBHE. The laminar flow at $300 \leq Re \leq 800$ [22] is the effect of tube separation [167]. The results were provided in temperature contours, PB, and \bar{Nu} number. The HRSG investigated the uniform rate of CHTC with each row of the TBHE and conducted a complete numerical study by [168] at $200 \leq Re \leq 2000$. The result shows that the impact of transverse pitch can be included as a bigger Re number in the lower cross-section. The effect of the longitudinal spacing on characteristics of CHTC in the in-line TBHE for a single phase with CFD was studied by [169]. The result shows that the turbulence model on characteristics of CHTC is increased.

3.5 The effect of fins pitch

An analytical study was conducted for a TBHE to reduce the thermal resistance and pressure gradient using the Darcy flow model. The model used two types of fins: parallel and annular fins. When observing a TBHE, the optimal design was obtained using the variables pitch, fin height, and spacing [170]. Empirical results show that the allowable ranges of decreasing the space between fins depend on the velocity flow and flow turbulence in the channel between fins [171]. The density ($1/p_F$)

ranged from 114 to 811fins/m geometrical parameters were identical for high CHTC and law PD [172]. The friction drag force is the total of the drag on a bare tube (Δp_T) and the drag caused by the fins (Δp_F), as suggested by [172]. The drag force on the fins is the difference between the total drag force and the force related to the corresponding bare tube banks. Hence, the FF from the fins is:

$$f_F = (\Delta p - \Delta p_T) \frac{2A_{cF} \times \rho}{(\dot{m})^2 A_F} \quad (1)$$

The FF and j -factor ($StPr^{2/3}$) are represented in Fig. 3 as a function of the Reynolds number based on D_h for the eight-fin spacing tested. Fig. 4 represents the fin FF calculated by Eq. (1) plotted against the Reynolds number based on the longitudinal row pitch, P_L , and the same j -factor [173]. To determine the effect of the number of tube rows on the j -element, similar HE geometry with 551 fins/m is used in a study performed later. The average j -factor for each exchanger as a function of Re_{PL} can be seen in Fig. 5 [174]. Many studies have been carried out on plain TBHE, stating that friction does not depend on number of rows [175-183]. Ward and Young reached A similar conclusion: the increase of fin spacing from 201.97 to 407.87 fins/m lead to decreases in PD [184]. Also, the pitch effect on CHTC and PD of TBHE with two rows experimentally [185]. A three-dimensional, laminar flow, incompressible and steady state of PD and HT in oval tube TBHE was studied. The effect of the fin parameter on the thermofluids characteristics for the Re number range of $100 \leq Re \leq 500$. The results showed that the efficiency depends on the fin parameter [186,187].

Sheui et al. have A the 3-D numerical for air flow over circular tubes TBHE studied. The PD and CHTC characteristics have been investigated. The results showed that adding fins leads to enhanced CHTC but causes an increase in PD [188]. The impact of geometry parameters on PD and CHTC for TBHE was carried out numerically [189]. According to this study, the main results are that the CHTC increases with increases ellipticity of the tubes. The CHTC on a TBHE with one fin-tube for several fin spacing was estimated numerically and experimentally [190]. The FDM and experimental data of temperature to predict the CHTC and fin efficiency are used. This study shows that the CHTC on the downstream fin is less than on the upstream fin. The effect of fin space and air velocity on mean CHTC for staggered TBHE was studied experimentally [191] as expected that the CHTC

increased with the increase in fin spacing and flow rate.

Huang et al. An SDM with CFX4.4, 3-D inverse problem in finding the CHTC for plain TBHE. The effects of fin pitch and air velocity were studied. The mean CHTC is greater than 8%-13% in the staggered arrangement compared with the in-line arrangement [192]. The effect of fin pitches on the CHTC for the TBHE in the range of $500 \leq Re \leq 800$ studied experimentally. The experimental study of thermal and flow characteristics for elliptic TBHE with an eccentricity of tube 0.5 and the flow range of $200 \leq Re \leq 1500$ was presented by [194]. The results in local and \bar{Nu} number, friction, and Colburn j -factors are increased with increase Re .

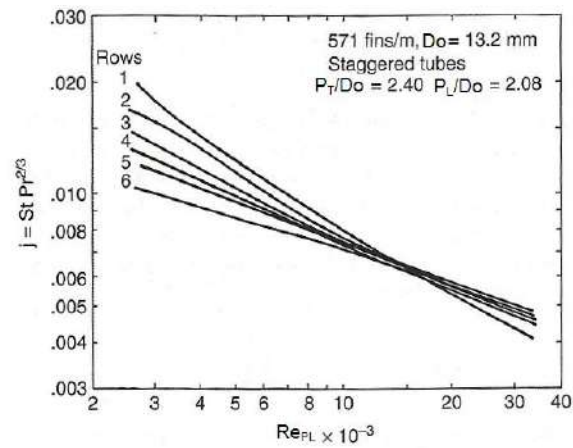


Figure 3: The HT and FF of a TBHE [98-173,99174].

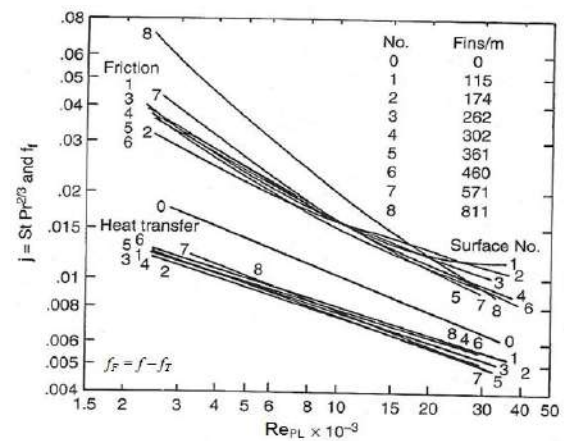


Figure 4: The effect of HT on TBHE [99-174,100-175].

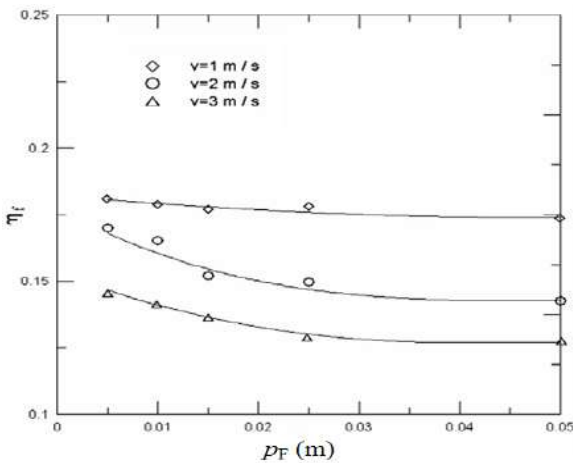


Figure 5: The j factor and FF with RePL [98,173,99,174].

4. Optimum spacing

Using available energy is the best solution to avoid the energy crisis in recent years. Using available energy (exergy) to improve industrial processes has been the most popular research topic. This is for using HEs in industrial applications because the optimal TBHE provides the maximum heat transfer for a given area. Such equipment should have high area density [195,196]. The maximum overall thermal conductance is proportional to $(\Delta P)^{0.5}$. The cooling used forced convection, the previous studies containing results of optimum space between parallel plates [197–199], and natural convection [200]. An experimental investigation of the effect of fin pitch on the CHTC at the circular pin fins with inline/staggered TBHE is investigated. The results show that the optimum space between fins is streamwise and spanwise at the shroud clearance and arrangement type used [201]. Later, previous work was extended by [202] and confirmed the optimum spacing between the tubes. He explained that this optimal spacing decreases with the Pr number, and the PD increases with the bundle length.

The experimental and numerical results for optimal spacing with the maximum thermal conductance are explained and correlated analytically by intersecting the small-spacing and large-spacing asymptotes of the thermal conductance function [203-205] and extending the previous work for the 3-D numerical and experimental. In the two Reynolds numbers based on swept length, Re_L is 852 and 1065. The main results from this study are the gain of heat transfer (thermal conductance) and reduction in relative material mass, which are up to 19 percent

and 32 percent, respectively [206]. Mainardes et al. A study has been done experimentally by forced convection for TBHE. The investigation was conducted for $2650 \leq Re \leq 10600$ with the ratio of tube spacing to minor diameter changed from 0.1 to 1.5. The result has shown the CHTC of up to 80% investigated when using an elliptical tube compared to a circular shape [207]. The study extended to parallel tubes in a solid matrix of fixed dimensions. The result was validated, and the case stated [208]. Investigations on the TBHE have been found in many different CFD codes, both in laminar and turbulent regimes. Design optimizations of HE were found in the size of tubes with the spacing and arrangements by different algorithms [209–214]. An experimental study has been done to reduce the power pumping in TBHE. [215]. The results presented at $2650 \leq Re \leq 10600$, tube pitch of $0.25 \leq P_T/2b \leq 0.6$, and eccentricities ranging from 0.4 to 1.0. The reduction in the pumping power is around 5%–10% at the elliptic TBHE compared with circular TBHE.

5. Correlations of thermo fluids

Several correlations, all based on experimental data for both average Nusselt number FF have been done.

5.1 Nusselt number

For CF over TBHE, the average Nusselt number is correlated by: [216,217].

The general form:

$$Nu_D = \frac{hD}{k} = C Re_D^m Pr^n (Pr/Pr_s)^{0.25} \quad (2)$$

Where:

C, m, and n depend on the value of the Reynolds number.

$$0.7 < Pr < 500 \\ 0 < Re_D < 2 \times 10^6$$

$$Nu_D = 0.9 Re_D^{0.4} Pr^{0.36} (Pr/Pr_s)^{0.25} \quad (3)$$

For (IL) $0 \leq Re_D \leq 100$

$$Nu_D = 0.52 Re_D^{0.5} Pr^{0.36} (Pr/Pr_s)^{0.25} \quad (4)$$

For (IL) $100 \leq Re_D \leq 1000$

$$Nu_D = 0.27 Re_D^{0.63} Pr^{0.36} (Pr/Pr_s)^{0.25} \quad (5)$$

For (IL) $1000 \leq Re_D \leq 2 \times 10^5$

$$Nu_D = 0.033 Re_D^{0.8} Pr^{0.4} (Pr/Pr_s)^{0.25} \quad (6)$$

For (IL) $2 \times 10^5 \leq Re_D \leq 2 \times 10^6$

$$Nu_D = 1.04 Re_D^{0.4} Pr^{0.36} (Pr/Pr_s)^{0.25} \quad (7)$$

For (staggered) $0 \leq Re_D \leq 500$

$$Nu_D = 0.71 Re_D^{0.5} Pr^{0.36} (Pr/Pr_s)^{0.25} \quad (8)$$

For (staggered) $500 \leq Re_D \leq 1000$

$$Nu_D = 0.35 (S_T/S_L)^{0.2} Re_D^{0.6} Pr^{0.36} (Pr/Pr_s)^{0.25} \quad (9)$$

For (staggered) $1000 \leq Re_D \leq 2 \times 10^5$

$$Nu_D = 0.031 (S_T/S_L)^{0.2} Re_D^{0.8} Pr^{0.36} (Pr/Pr_s)^{0.25} \quad (10)$$

For (staggered) $2 \times 10^5 \leq Re_D \leq 2 \times 10^6$

$$Nu_{D,N_L} = F Nu_D \quad (11)$$

Colburn suggested the correlation between flow and heat transfer over a staggered TBHE [218].

$$Nu = 0.33 \times Re^{0.6} Pr^{1/3} \quad (12)$$

For $N=10$, $10 < Re < 4 \times 10^4$.

The characteristics of heat transfer for both configurations in-line and staggered TBHE were carried out experimentally and based on a correlation of the empirical results [219].

$$Nu = C \times Re^n \quad (13)$$

For air and $N=10$.

Another correlation has been developed for the number of rows less than ten [220]. its correction C_2 , defined as:

$$C_2 = \frac{h_{N_R}}{h_{10}} \quad (14)$$

Where h_{N_R} and h_{10} the CHTC for $N_R < 10$

$$Nu|_{(N_R < 10)} = C_2 \times Nu|_{(N_R \geq 10)} \quad (15)$$

For $N_R > 10$

The correlation constants of C , C_2 , and n , are contained in tables; in most textbooks for heat transfer (e.g., [221-223]) for in-line/staggered TBHE.

A second way and to obtain the following expression [219].

$$Nu = 0.32 \times F_a \times Re^{0.61} Pr^{0.31} \quad (16)$$

The slight modification for the above Eq. (4) offered the new correction for staggered TBHE [224].

$$Nu = 0.35 \times F_a \times Re^{0.57} Pr^{0.31} \quad (17)$$

With

$$F_a = 1 + 0.1 \times P_L + \frac{0.34}{P_T} \quad (18)$$

For in-line TBHE

$$Nu = 0.34 \times F_a \times Re^{0.61} Pr^{0.31} \quad (19)$$

With

$$F_a = 1 + \left(P_L + \frac{7.17}{P_L} - 6.52 \right) \left\{ \frac{0.266}{(P_T - 0.8)^2} - 0.12 \right\} \left(\frac{1000}{Re} \right)^{1/2} \quad (20)$$

Additional use B.C at isothermal [132]. The analytical solution for heat transfer over TBHE the correlation as:

$$Nu = C_a \times Re^{1/2} Pr^{1/3} \quad (21)$$

can be employed with

$$\begin{aligned} \text{in-line TBHE} \quad C_a &= [0.25 + \exp(-0.55 \times P_L)] \times P_L^{0.212} P_T^{0.285} \\ \text{staggered TBHE} \quad C_a &= \frac{0.61 \times P_L^{0.053} P_T^{0.091}}{[1 - 2 \times \exp(-1.09 \times P_L)]} \end{aligned}$$

A mean Nu number for the whole TBHE an empirical correlation of the form:

$$Nu = C \times C_1 \times Re^m Pr^n \quad (22)$$

For $N > 16$

C , m , n , and C_1 in-line/staggered from textbooks [222,223].

Ref. [225] displayed the measurement values of heat transfer in the empirical correlations. For both in-line and SGs, they are correlated by [219] the measurements for each of the tests of [226] and Pierson [227]. This empirical correlation was related to tube bundles for 10 or more tube rows in the deep flow.

The experimental study of air flow over the in-line tube near a wall is presented by [228]. The range of Re number from $0.8 \times 10^4 \leq Re \leq 4 \times 10^4$, the clearance,

c ratio $0.05 \leq c \leq 4.0$, and the longitudinal pitch, P_2 is $1.2 \leq P_2 \leq 4.4$. The correlation of the overall Nu number:

$$Nu_m = 0.103 \times Re^{0.74} \left(\frac{P_2}{D} \right)^{-0.12} \left(\frac{c}{D} \right)^{0.23} \quad (23)$$

The deviation of correlation above about $\pm 5\%$ of in the ranges P_2/D is $1.2 \leq P_2/D \leq 3.2$, c/D is $0.18 \leq c/D \leq 0.16$, and Re is $0.8 \times 10^4 \leq Re \leq 4 \times 10^4$

5.2 Friction Factor

Another correlation to predict the j and f factor versus Reynolds number for plain on staggered tube arrangement was studied in [217].

$$\Delta P = N_L f_X \frac{\rho^{\circ} V_{max}^2}{2} \quad (24)$$

FF f and correction factor for both IL and staggered TBHE as in fig.6 (a,b).

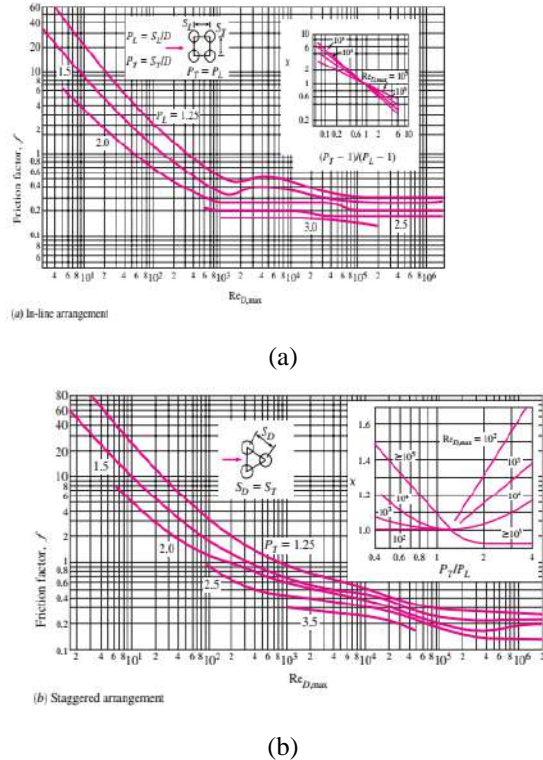


Figure 6: shows FF f and correction factor for tube banks [217].

The heat transfer for four or more tube rows of staggered tube geometry is correlated by [229].

$$j_4 = 0.14 \times (Re_D)^{-0.502} \left(\frac{S_F}{D_o} \right)^{0.031} \left(\frac{P_T}{P_L} \right)^{-0.502} \quad (25)$$

The assumption made in Eq. (14) is that the fourth row stabilizes the heat transfer coefficient, so in case of more than four tube rows and less than four, the j -factor is governed by the correlation as shown:

$$\frac{j_{NR}}{j_4} = 0.991 \times \left[2.24 \times (Re_D)^{-0.092} \left(\frac{N_R}{4} \right)^{-0.031} \right]^{0.607 \times (4-N_R)} \quad (26)$$

Eq. (16) gives the FF of the HE [229].

$$f = f_F \frac{A_F}{A} + f_F \left(1 - \frac{A_F}{A} \right) \left(1 - \frac{t_F}{p_F} \right) \quad (27)$$

And:

$$f_F = 0.508 \times (Re_D)^{-0.521} \left(\frac{S_F}{D_o} \right)^{1.318} \quad (28)$$

A higher FF is predicted by [230,231] for three or more tube rows; the correlation is:

$$j_3 = 0.163 \times (Re_d)^{-0.369} \left(\frac{s}{d_o} \right)^{0.0138} \left(\frac{P_T}{d_o} \right)^{0.13} \left(\frac{P_T}{P_L} \right)^{0.106} \quad (29)$$

$$N_R \geq 3 \quad (29)$$

$$\frac{j_{NR}}{j_3} = 1.043 \times \left[(Re_D)^{-0.564} \left(\frac{S_F}{D_o} \right)^{-0.123} \left(\frac{P_T}{D_o} \right)^{1.17} \left(\frac{P_T}{P_L} \right)^{-0.564} \right]^{(3-N_R)} \quad (30)$$

$$N_R = 1, 2 \quad (30)$$

$$f_F = 1.455 \times (Re_D)^{-0.656} \left(\frac{S_F}{D_o} \right)^{-0.134} \left(\frac{P_T}{D_o} \right)^{1.23} \left(\frac{P_T}{P_L} \right)^{-0.347} \quad (31)$$

For the FF due to tubes, f_T , which is shown by [232]:

$$f_T = \frac{\pi}{4} \left\{ 0.25 + \frac{0.188}{\left(\frac{P_T}{D_o} - 1 \right)^{1.08}} (Re_D)^{-0.16} \right\} \times \left[\frac{P_T}{D_o} - 1 \right] \quad (32)$$

The FF of the HE is calculated by Eq. (16).

Another correlation suggested by [233] for the estimation of Sherwood number and friction loss is as follows:

$$\left. \begin{aligned} \overline{Sh} &= c \times Re^n \quad Sc^{0.333} \\ f &= c \times Re^n \end{aligned} \right\} \quad (33)$$

The correlations parameters c and n are tabulated in Table 2.

For $100 \leq Re \leq 500$.

The Nu number correlation is defined as [234]:

$$Nu = 1.565 \times Re^{0.3414} \left(N_R \times \frac{P_F}{D_o} \right)^{-0.165} \left(\frac{P_2}{P_1} \right)^{0.0558} \quad (34)$$

Elsewhere, the FF correlation is given by the equation

$$f = 20.713 \times Re^{-0.3489} \left(N_R \times \frac{P_F}{D_o} \right)^{-0.1676} \left(\frac{P_2}{P_1} \right)^{0.6265} \quad (35)$$

For more correlations were summarized in Table 2 [103].

6. Flat tubes and other shapes

Flat tubes are a relatively modern technology used in various engineering applications, such as modern HEs and car radiators. The main objective of using HEs is to obtain the largest amount of heat exchange in return, taking into account the following variables: PD and the consequent provision of pumping power, volume, cost, vibration, noise, and the type of metal used. Many researchers have devoted their work to studying fluid flow and heat transfer over cylindrical bodies. An experimental of HT and fluid flow over an FT are investigated for $124 \leq Re \leq 622$. The uniform HF supplies are 354.9, 1016.3, and 1935.8 W/m², respectively. The experimental results indicate that the average Nu increases with Re and heat flux supply. The FF decreased with increases of Re [235]. Flat tubes have not been investigated as much as they provide space for heat transfer and improve the performance of TBHE [236-244]. Compared to the circular tube TBHE, flat tube TBHE is expected to have lesser air-side PD and improved air-side CHTC. The same reason contributes to smaller vibration and noise in flat tube HEs than in circular tube HEs [245].

6.1 In line and SGs

The previous literature on the CHTC and PD over the flat TBHE is very little, excluding the contemporary studies of [246-248]. A numerical steady, laminar, incompressible, 2-D flow over a TBHE for both in-line and staggered has been investigated [246]. Another study presented the results for the 2-D, incompressible and unsteady flow over in-line/staggered TBHE is flux and isothermal B.C. From the standpoint of the HT, the in-line better than that staggered for most of the cases. While the PD is higher for in-line compared with the staggered TBHE [247]. A numerical studied of the HT and PD over a TBHE had been estimated. The results show that the CHTC and PD increase with an increase of Re always [249,250]. An experimental study for TBHE with both oval and circular shapes was carried out. The value CHTC is equal in both shapes. While the PD is lower than 10% in the oval shape [251,252]. Tahseen et al. have conducted an experimental investigation of the thermofluids characteristics of airflow in-line TBHE for laminar and incompressible. The results were presented in \overline{Nu} numbers, PD increases with increases Re [253]. Numerical studies for the PD and CHTC in the TBHE with staggered, circular, wing-shaped, and elliptic are studied [254-256]. The results of all

studies showed the difference between C_d and \overline{St} the number of a few at an increase hydraulic diameter. Wang et al. [257] A numerical and experimental to get the performances of CHTC in TBHE has been studied. The deviation in the average CHTC obtained from two ways of the B.C are higher than 5% for fin efficiency less than 80. An experimental study has been made to investigate CHTC and PD around TBHE with $527 \leq Re \leq 880$ and $Pr=0.71$ and various HF. The study results indicate that the The average Nusselt number of all flat tubes has increased by 23.7%-36.7% as Reynolds numbers vary from $527 \leq Re \leq 880$ at the fixed heat flux [258].

6.2 Rows of tubes between two plates

The used of HEM to obtain the distribution of temperature and CHTC over TBHE was carried out numerically from [259]. For $50 \leq Re \leq 500$ with three pitches, H/D of 1.5, 2.0, and 3.0, and tube pitches, L/D of 2.0, 3.0, and 6.0. The bulk temperature rises almost linearly from one HEM to another HEM for an equal rate of HT. In the same year, another studied PD and CHTC [260]. In the flowing year [261] conducted, an experimental study for the PD and CHTC for TBHE at $220 \leq Re \leq 2800$. Compared numerical results with [262]. A similar numerical analysis for flat TBHE was carried out by [263] using the FVM to solve the equations of motions and the BFC at $25 \leq Re \leq 300$, longitudinal pitches of 2, 3, and 4 at the Pr are taken 0.7. The PD and CHTC across-flow through TBHE were studied by [264]. The equations of motions were solved by using the FVM $100 \leq Re \leq 300$ and $0.5 \leq \text{gap/diameter} \leq 1.25$. The value \overline{Nu} would have been indicated along cylinders.

7. Constructal theory

The constructal theory is considered one of the most important applications in the field of engineering; the use of design with constructal theory in the design of HEs in order to obtain the optimal area density, which is considered one of the most important design determinants of HEs because size has a major role, regardless of cost, weight or performance. Recently, researchers tended to apply the above theory. The research in this field can be divided into single and multiple scales and can be summarised in table 3 [265].

8. Future work

A longitudinal fin TBHE is one of the most critical essential components, commonly used recently in

automobile radiators, refrigeration devices, condensers, and other uses. The size of the TBHE has an effective role in engineering applications. If a comparison is made between the flat and round TBHE, we find a large difference that may reach three times the size of the flat tube at the same operating conditions. In addition, flat TBHE has lower-side air PD and improved CHTC. For the above reasons, The optimal Flat tube with front fin, flat tube with rear fin, flat tube with front and rear fin, the distance between two rows of longitudinally TBHE, the distance between two columns, and the effect of the angle of inclination of the rear fins with maximum total CHTC and minimum PD needs further focus and research in Future study.

9. Conclusions

A comprehensive review has been done in the field of finned and non-finned TBHE and a review of different designs of tubes (circular, longitudinal, or flat). The main determinant for choosing the optimal design is to improve the CHTC, but the PD depends on the design. Therefore, we must focus on an important matter: when the PD is essential, it is in a high range of Reynolds numbers. In order to agree between the variables affecting the Reynolds number, the effect of fluid velocity, pipe shape, the horizontal and vertical distance between pipes, spacing, and shape of fins was reviewed.

Through the review of previous research, the main conclusions can be established as follows:

- CHTC and PD are a function of the Reynolds number.
- The effect of circular tube TBHE has been documented by a few studies, unlike the flat tube.
- The SG shows a higher CHTC compared to the IL configuration.
- The CHTC and PD increase with the number of fins.
- The tube shape and arrangement clearly affect CHTC and PD.
- Eventually, to obtain a HE with high efficiency, i.e., high CHTC and low PD, studies must focus on this field.

Acknowledgments

After completing this research, the authors would like to express their gratitude to the Presidency of Tikrit University, the Deanship of the College of Engineering, and the Presidency of the Department of Mechanical Engineering. I would also like to thank the presidency of the Northern Technical University and the Deanship of the Technical Institute, Hawija, for their work facilitation.

Table 1 Effect of the flow and geometric parameters on the thermofluids characteristics.

NO	Researcher	Type	Re number and velocity range	Tube shape	Geometric parameter	Finding
1	Tutar and Akkoca [88]	N	$600 \leq Re \leq 2000$	Cir	$0.116 \leq Pf \leq 0.365$	<ul style="list-style-type: none"> • The small effect of the number of tube rows on the heat transfer coefficient when the number of multi-rows $N_g > 4$. • The PD increased with the number of rows from 1 to 4 for both IL and SGs.
2	Paeng et al. [105]	N +E	$1082 \leq Re \leq 1649$	Cir.	OD=10.2mm, $Pf=3.5$ mm	<ul style="list-style-type: none"> • The deviation between these experimental results and previous work is 7-32.4%. • The error range in the correlation of 16.5-31.4% with compared previous correlation.
3	Ibrahim and Gomaa [113]	N+E	$5.6 \times 10^3 \leq Re \leq 4 \times 10^4$	Elp.	$0.25 \leq A \leq r1.0$	<ul style="list-style-type: none"> • The better thermal performance with a smaller Re number and Ar. • The HE employing elliptic tube arrangement contributes significantly to the energy conservation
4	Simo Tala et al. [114]	N	Re=1050, and 2100	Cir. Elp.	e = 1.0(circular); e=0.7 and e=0.5	<ul style="list-style-type: none"> • The increase of thermal-hydraulic performance of above 80% was obtained with a reduction in the tube ellipticity compared with a circular-shaped tube. • The reduction of the thermal and viscous irreversibilities respectively down to 15% and 50% was observed in the modified shapes when compared to circular ones
5	Yan and Sheen [115]	E	$300 \leq Re \leq 2000$	Cir.	$P_L=19.05$ mm; $P_T=25.4$ mm; $P_f=1.4, 1.69, \text{and} 2.0$	<ul style="list-style-type: none"> • The $\Delta \tilde{P}$ increased with increases in the number of tube rows for the same frontal air velocity
6	Halici et al. [116]	E	$0.9 \text{ m/s} \leq u \leq 4 \text{ m/s}$	Cir .	Rowno. = 1-4	<ul style="list-style-type: none"> • The increase in the number of tube rows leads to a decrease in the Colburn j and FFs
7	Kim et al. [117]	E	$550 \leq Re \leq 1200$	Cir	$P_L = 27, 30, \text{and} 33$ mm mm $P_f = 7.5, 10.0, 12.5, \text{and} 15.0$	<ul style="list-style-type: none"> • The staggered fin and tube configurations enhance heat transfer performance by 7% and 10%, respectively, compared to the IL fin configuration. • The heat transfer performance decrease with the increase of tube number
8	Yoo et al. [118]	E	$7.7 * 10^3 \leq Re \leq 30.3 * 10^3$	Cir	$P_L = P_T = 1.5, 1.75, \text{and} 2.0$	<ul style="list-style-type: none"> • The Nu number increases by more than 30% and 65% on the second and third tubes, respectively, compared with the first. • The local heat transfer coefficients on each tube increase except on the front part of the first tube as the tube spacing decreases
9	Beale and Spalding [119]	N	$100 \leq Re \leq 1000$	Cir	$1.25 \leq p/D \leq 2.0$	<ul style="list-style-type: none"> • The results were shown in the form of the friction coefficient, PD, and coefficient of heat transfer
10	Khan et al. [120].	A	$1 \times 10^3 \leq Re \leq 1 \times 10^5$	Cir	$PL = 20.5, \text{and} 34.3$ mm $PT = 20.5, \text{and} 31.3$ mm	<ul style="list-style-type: none"> • The \tilde{Nu} numbers depend on the transverse, longitudinal pitches, and Reynolds numbers. • For SG, the heat transfer coefficient is higher compared with the IL configuration

11	Xie et al. [121].	N	$1 \times 10^3 \leq Re \leq 6 = 10^3$	Cir	$32 \text{ mm} \leq P_L \leq 36 \text{ mm}$, $19 \text{ mm} \leq P_T \leq 23 \text{ mm}$	<ul style="list-style-type: none"> The decrease in the transverse pitch causes an increase in flow velocity, which in turn enhances the heat transfer. The heat transfer and flow friction of the presented HEs are correlated in the multiple forms
12	Ramana et al. [122]	E	$200 \leq Re \leq 1500$	Cir	$P_L = P_T = 2.0$	<ul style="list-style-type: none"> The high Reynolds number enhancement of the heat transfer is 100% with the SG. The PD in an IL arrangement decreased by about 18% compared to configurations without the porous medium.
13	Berbish [123]	N +E	$4000 \leq Re \leq 45570$	Elp.	$1.5 \leq P_L, P_T/b \leq 4.0$	<ul style="list-style-type: none"> For $Re < 14100$, the large local Nusselt number takes place at the leading edge (e.g., $P/b = 0.0$). For $Re > 414100$, the maximum value of the average Nusselt number enhancement ratio is nearly about 2.0
14	Lee et al. [124]	N	$500 \leq Re \leq 2000$	Cir.	$3.0 \leq PT \leq 7.0$	<ul style="list-style-type: none"> The impact of the transverse pitch in the higher Reynolds numbers on the drafting of the traditional heat transfer. Increasing the longitudinal space for the uniformly distributed cylinders will strengthen the total heat transfer. Otherwise, the maximum \tilde{N}_u number is the without-uniformity temperature on the wall fin and tube wall.
15	Chen et al. [125]	N	$100 \leq Re \leq 500$	Elp.		<ul style="list-style-type: none"> The heat transfer ratio of tube surface to fin was still $< 10\%$. The fin efficiency and fin temperature depend slightly on the fin parameters.
16	Sheui et al. [126]	N	$0.3 \leq u \leq 2.0$	Cir.	$0.4 \leq p_f \leq 5.0$	<ul style="list-style-type: none"> The addition of fins leads to enhanced heat transfer but causes an increase in the PD.
17	Erek et al. [127]	N	the mass flow rate used in all of the models is $1.904 \times 10^{-5} \text{ kg/s}$	Cir.	$P_L = 35, \text{ and } 38$	<ul style="list-style-type: none"> The heat transfer increases with the increasing ellipticity of the tubes. However, the PD is significantly reduced by increasing tube ellipticity and decreasing the density of fins.

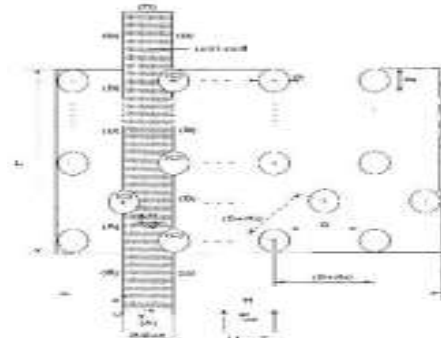
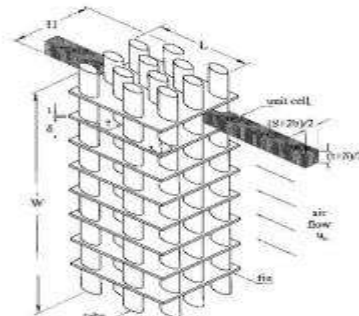
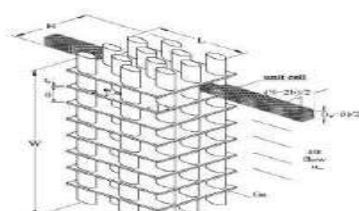
Table 2 Details more correlations with condition and geometry parameters.

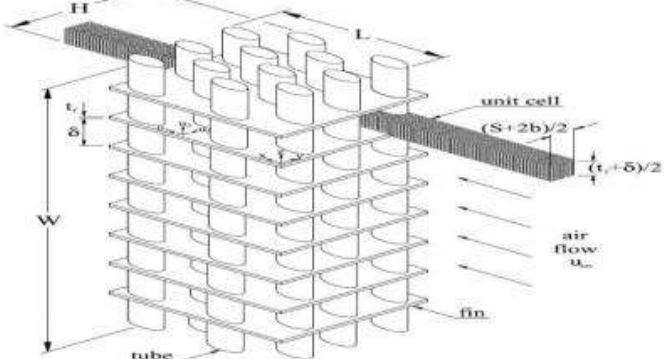
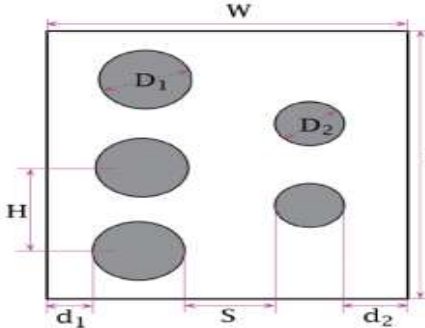
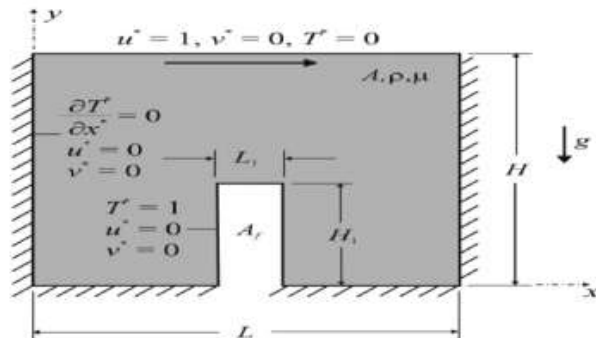
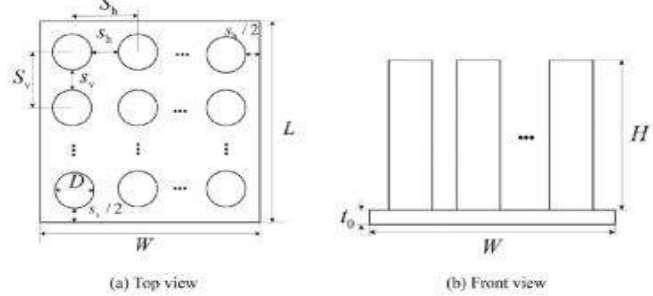
NO	Researchers	Correlations	Conditions	Geometry parameters	Method	Tube shape	Deviation (%)
1	Taler [66]	$Nu_a = 0.1386 \times (Re_a)^{0.6103} (Pr_a)^{1/3}$	$155 \leq Re_a \leq 331$	In–lin.	S + E	Elp.	–
		$j_a = 0.1386 \times (Re_a)^{-0.3897}$					
2	Paeng et al. [105]	$Nu = 0.049 \times (Re_D)^{0.784} (Pr_f)^{1/3}$	$1082 \leq Re_D \leq 1649$	Stagg.	N + E	Cir.	0.4–6.0
3	Taler [108]	$Nu_a = 0.06963 \times (Re_a)^{0.6037} (Pr_a)^{1/3}$	$200 \leq Re_a \leq 1500$	In–lin.	N	Elp.	

4	Rosman et al. [118]	$\overline{Nu} = [3.58 + 8.46 \times 10^{-4} Re^{1.24}] \times Pr^{0.4}$	$200 \leq Re \leq 1700$	In-lin.	T+E	Cir.	2.5
5	Xie et al. [146]	$Nu = 1.565 \times Re^{0.3414}$ $\times \left(\frac{P_T}{P_L} \right)^{0.0558} \left(N_R \frac{p_F}{D_o} \right)^{-0.165}$	$1 \times 10^3 < Re < 6 \times 10^3$ $16 \text{ mm} \leq D_o \leq 20 \text{ mm},$ $2 \text{ mm} \leq p_F \leq 4 \text{ mm},$ $38 \text{ mm} \leq P_T \leq 46 \text{ mm},$ $32 \text{ mm} \leq P_L \leq 36 \text{ mm}$	Stagg.	N	Cir.	3.7
		$f = 20.713 \times Re^{-0.3489}$ $\times \left(\frac{P_T}{P_L} \right)^{0.6265} \left(N_R \frac{p_F}{D_o} \right)^{-0.168}$					6.5
6	Kayansayan [171]	$j = 0.15 \times Re^{-0.28} \left(\frac{A_o}{A_{to}} \right)^{-0.362}$	$5 \times 10^2 < Re < 3 \times 10^4,$ $11.2 \leq A_o/A_{to} \leq 23.$	Stagg.	E	Cir.	8.2
7	Chen and Ren [176]	$Nu = 0.191 \times Re^{0.68} Pr^{0.4}$	$4.5 \times 10^3 \leq Re \leq 2.7 \times 10^4,$ $0.336 \leq H/D \leq 0.516$	Stagg.	E	Cir.	5
8	Colburn [207]	$Nu = 0.33 \times Re^{0.6} Pr^{1/3}$	$10 \leq Re \leq 4 \times 10^4,$ $N_R \geq 10$	—	—	Gen.	—
9	Taler [224]	$Nu = 0.085 \times Re^{0.712} Pr^{-1/3}$	$150 \leq Re \leq 350$	Auto. radiator	E	Elp.	—
10	Dittus and Boelter [225]	$Nu = 0.023 \times Re^{0.8} Pr^{0.3}$	$Re \geq 1 \times 10^4,$ $0.7 \leq Pr \leq 100,$ $L/D \geq 60$	Auto. radiator	E	Gen.	—
11	Merker and Hanke [226]	$Sh = 1.181 \times Re^{0.480}$	$P_L = 1.0,$ $1.97 \leq P_T \leq 3.16,$ $Re < 6400$	Stagg.	E	Elp.	—
		$Sh = 1.212 \times Re^{0.676}$	$Re > 6400$				—
12	Chen and Wung [227]	$Nu = 0.8 \times Re^{0.4} Pr^{0.37}$	$40 \leq Re \leq 800,$ $0.1 \leq Pr \leq 10$	In-lin.	A	Cir.	—
		$Nu = 0.78 \times Re^{0.45} Pr^{0.38}$		Stagg.			—
13	Wang et al. [228]	$Nu = 1.7 \times Nu_Z$	$N_R > 1,$ $Re < 500$	Stagg.	E	Cir.	5.9
		$Nu = 1.38 \times Nu_Z$	$N_R > 1,$ $500 < Re < 1000$				—
14	Kim and Kim [229]	$j = 0.710 \times Re_{Dh} \times N_R^{-0.141} p_F^{0.384}$	$600 \leq Re_{Dh} \leq 2000,$ $7.5 \leq p_F \leq 15,$ $1 \leq N_R \leq 4$	In-lin.	E	Cir.	3.8
				Stagg.	—	—	6.2
15	Khan et al. [230]	$Nu = 0.33 \times Re^{0.64} Pr^{1/3}$	$1 \times 10^4 \leq Re \leq 3.6 \times 10^4$	In-lin.	E	Elp.	14.5

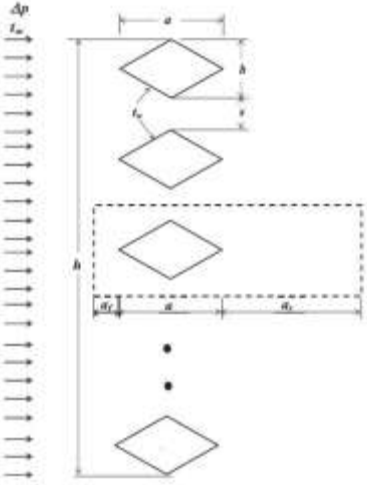
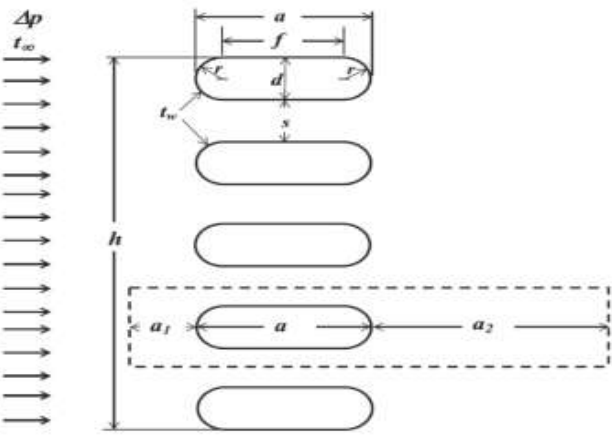
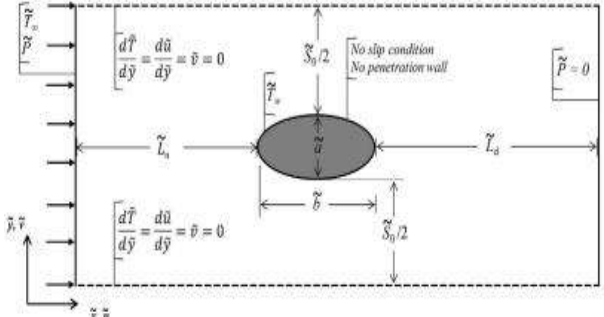
16	Jacimovic et al. [231]	$f = \left(\frac{180}{Re^{0.85}} + 0.52 \right) \times R_d^{0.65} W^{-0.7}$	$300 < Re < 4000$	Stagg.	E	Cir.	5.7
(Auto.: automotive; A: analytic; Cir: circular tube; E : empirical; Elp.: elliptic; N: numerical; In-lin.: in-line; S: simulation; Stagg.: staggered)							

Table (3): Summary of Literature Survey with DCT.

NO	Authors	Configuration	Range	Conclusions
1	Matos [22]		$300 \leq Re \leq 800$	Elliptical 13%: Gain of heat transfer Circular 25% reduction in PD concerning previous studies.
2	Matos [205]		$852 \leq Re \leq 8520$	Elliptic arrange. Enhancement of 20% as compared with circular arrange.
3	Matos et al. [206]		$852 \leq Re \leq 1065$	An enhancement of 19% was obtained with elliptic TBHE, which was accompanied by a reduction in circular TBHE of 32%

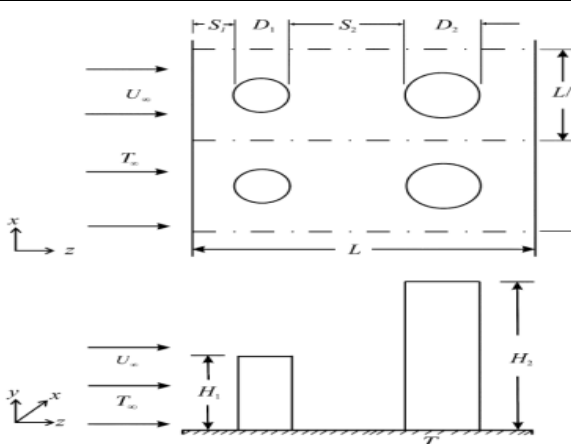
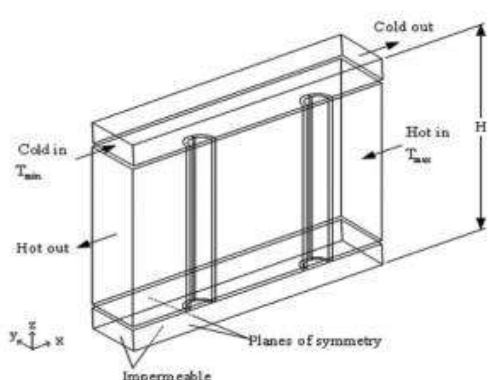
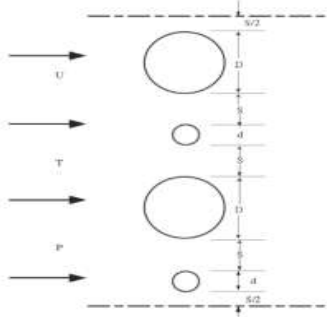
NO	Authors	Configuration	Range	Conclusions
8	R. L. S. Mainardes et al. [215]		$Re = (2650, 5300, 7950, \text{ and } 10600)$.	Utilizing constructal design with elliptic configuration reduces pumping power by (10%) with optimum spacing distance, eccentricity, and dimensional fin density of (0.5, 0.5, and 0.006) respectively.
9	Gongnan Xie [270]		$Be = 0, 0.5, 1$	Adopting entropy generation minimization and constructal law as a mutually coupled technique for the utilized pin fin exchanger increases thermal energy stored by (10.2%).
10	G. Lorenzini et al. [271]		$Ra = (10^3, 10^4, 10^5, 10^6), (Re = (10, 10^2, 3 * 10^2, 5 * 10^2, 7 * 10^2, 10^3))$.	Fin aspect ratio largely affects fin Nusselt number with a considerable change for different values of Rayleigh numbers.
11	Lingen Chen [272]		$10^2 \leq Re \leq 10^5$	The optimum fin diameter based on constructal design maximizes heat density with decreasing dimensional pressure difference for a given heat sink shape. The PD was found to increase with increases in fluid velocity.

NO	Authors	Configuration	Range	Conclusions
12	G.M. Barros et al [273]		$Ri = (0.1, 0.5, 1, 5, 10)$, $(Re = 100)$	Maximum Nusselt number observed with a transverse pitch to cylinder diameter of (5) and (2.5) for Richardson numbers of (0.1 and 10), respectively.
13	Ahmed Waheed et al. [274]		$Ra = 10^3, 10^4, \text{ and } 10^5$	The optimum spacing distance at a given Rayleigh number remains constant for all tube diameters. The results also showed that for the same Rayleigh number and space size
14	A.L. Razera [275]		$Re \text{ & } Ra = (10, 10^2, \text{ and } 10^3) \text{ and } (10^3, 10^4, 10^5, \text{ and } 10^6)$	The optimum shape was found to have a thermal performance gain of (40%) in comparison with other proposed geometries.
15	Ahmed Waheed [276]		$Rayleigh number (10^3 \leq Ra \leq 10^5)$	With the increasing Rayleigh number, the optimum distance decreases in accordance

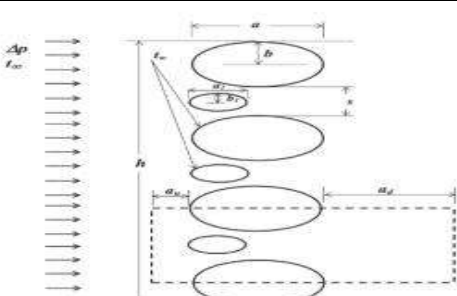
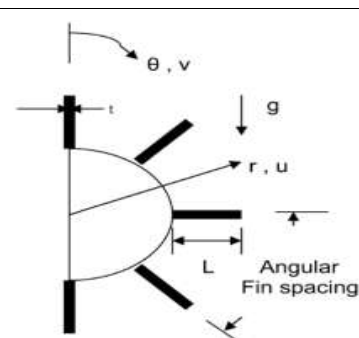
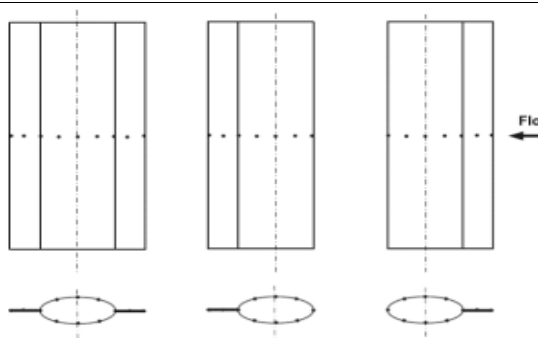
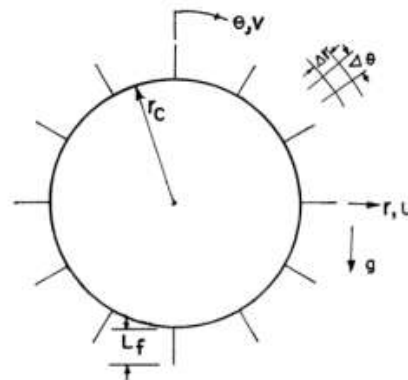
NO	Authors	Configuration	Range	Conclusions
16	Ahmed Waheed [277]		$10^3 \leq Be \leq 10^5$	With the decreasing of optimum spacing, heat density increases to a maximum value as the Bejan number is raised for all tubes' vertical axes
17	Ahmed Waheed [278]		$10^3 \leq Be \leq 10^5$	The decreasing of tube flatness with a constant Bejan number leads to the lowering of the optimum heat density
18	A.L. Razera et. Al,[279]		$Be = 10, \text{ and } 5 \times 10$	Optimization with a constructal design enhanced heat density in the range of (50% to 97%) as compared with cases that utilize fewer degrees of freedom

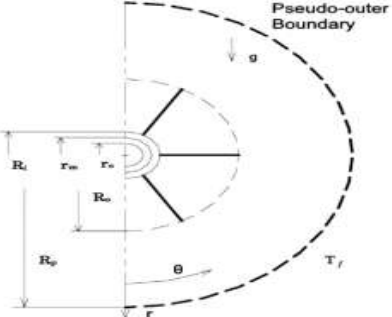
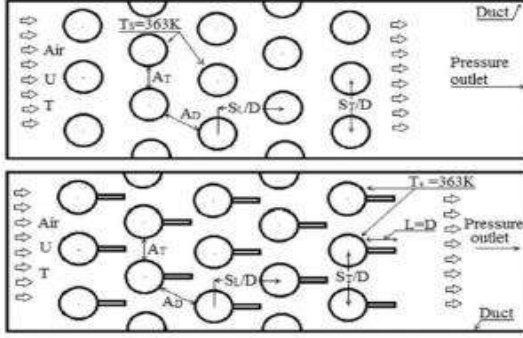
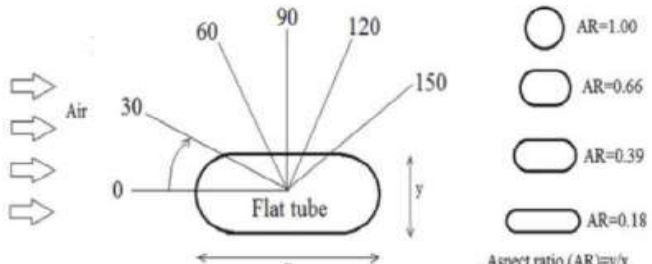
NO	Authors	Configuration	Range	Conclusions
19	A. Bejan [280]		$10^3 \leq Be \leq 100*10^9$	The unused flow region can be filled with smaller blades to produce a more efficient system.
20	T. Bello-Ochende [281]	 	$10^5 \leq Be \leq 10^8$	The performance-enhanced as system complexity increases and as the number of rated Fins increases to three and the optimal length of Fins increases with the Bejan number increases.
21	T. Bello-Ochende et. Al, [282]		$10^3 \leq Be \leq 10^6$	The flow structure gets less permeable as the number of Fins grows, and the flow rate falls. Also, the overall heat transfer rate density rises

NO	Authors	Configuration	Range	Conclusions
22	Alexandre K. da Silva [283]		$10^7 \leq Ra \leq 10^8$	Once the complexity regarding flow structure is optimized, then the rate of heat transfer density was found to be maximized.
23	T. Bello-Ochende et. Al [284]		$10^3 \leq Ra \leq 10^5$	The spacing between large-scale cylinder increases by irrigating the small cylinders in the unheated region. When the flow grows faster, spacing becomes smaller, while the cylinders' diameters reveal a minor change.
24	T. Bello-Ochende et. Al [285]		$10^5 \leq Be \leq 10^7$	Results were in fair agreement with foretelling analytical outcomes

NO	Authors	Configuration	Range	Conclusions
25	T. Bello-Ochende et. Al [286]		Re = 50	The optimal configuration for a pin fin obtained between (0.05) and (0.2) for short Fins while a ratio of pin fins diameters varied in the range of (1) and (1.2), and a ratio of the large fin to small fin height range from (0.9) and (1.2).
26	Y. Kim [287]		Gr = 10^4 Re = 500	For the three vertical tubes (better to include the spacing distance between tubes). For four tubes (The case of two vertical tubes of almost the same diameters is better in performance)
27	T. Bello-Ochende et. Al [288]		10 ≤ Be ≤ 10^4	Enhancements were found influential in the case of rotating cylinders aligned on the same axis of rotation rather than in the case of cylinders aligned on the plane of the leading edge.

NO	Authors	Configuration	Range	Conclusions
28	H. Kobayashi [289]		None	Asymmetry in the morphing and evolution of the tree shape configuration led to better optimum design
29	H. Matsushima et. Al [290]	<p>Fig. 1. Conductive base with non-uniform thickness and uniformly spread gas for convection.</p>	None	Optimal spacing and height are found for cases that maximize the heat transfer rate and connect optimum heat transfer with the spacing distance between fins in the constructal design.
30	Page et. Al [291]		$10^1 \leq Ra \leq 10^4$	The rotation of cylinders did not influence maximum heat transfer density compared to a stationary case at large values of Rayleigh numbers. Optimum spacing was found to be decreased with the increase of cylinders' rotational speed.
31	Ahmed Waheed [292]		$10^4 \leq Be \leq 10^6$ $0.1 \leq Ra/Be \leq 10$	Utilizing multi-scale arrangement enhanced heat transfer density twice that of the single-scale arrangement

NO	Authors	Configuration	Range	Conclusions
32	Ahmed Waheed et. Al [293]		$10^3 \leq Be \leq 10^5$	When the smaller tubes are irted between, the bigger tubes, the heat transfer rate is increased for different semi-minor axes of the larger tubes.
33	Haldar et. Al [294]		$Gr = 10^5$	Maximum heat transfer can be obtained with thin fins of (0.01 m), optimum fin number of (6), and optimum fin length of (0.2 m)
34	Ibrahim [295]		$Re = (4.75 \times 10^3) \text{ to } (3.96 \times 10^4)$	irreversibility ratio, FF, and the coefficient of heat transfer affected by the position of the fin concerning the elliptic tube surface
35	HALDAR [296]		$10^2 \leq Gr \leq 10^6$	As the Grashof number increases, which is accompanied by an increase in both fins number and length, the heat transfer rate also increases

NO	Authors	Configuration	Range	Conclusions
36	J. M. WU et. Al [297]		Ra = 7120	For fins numbers (4 to 10), fin efficiency decreases with increasing fins number. Numerical results for eight fins configuration reveal that there should be no fins aligned in the vertical plane.
37	Chidanand K. Mangrulkar et al. [298]		Re = 5500 to 14,500	Adding a splitter Fin to a fluid flow raises the Nusselt number, heat transfer, and lowering PD within the tube bank compared to a bare cylinder.
38	Chidanand K. Mangrulkar et. Al [299]		Re ≤ 8000	At fixed mass flow, greater enhancements are attained with increased diameter unfinned tubes but at a high penalty in PD and pumping power.

References

[1] Brauer H. Compact HEs. *Chem Proc Eng* 1964;45:451–60.

[2] Manglick RM. Heat transfer enhancement. In: Bejan A, Kraus DA, editors. *Heat transfer handbook*. New York: Wiley; 2003.

[3] Optimal geometric arrangement of unfinned and finned flat tube HEs under laminar forced convection T.A. Tahseen PhD. Thesis, Universiti Malaysia Pahang (UMP) 3, 2014

[4] Zukauskas. “Heat Transfer from Tubes in CF.” In *Advances in Heat Transfer*, ed. J. P. Hartnett and T. F. Irvine, Jr. Vol. 8. New York: Academic Press, 1972.

[5] Beale SB, Spalding DB. A numerical study of unsteady fluid flow in in-line and staggered tube banks. *J Fluids Struct* 1999;13:723–54.

[6] Wilson AS, Bassiouny MK. Modeling of heat transfer for flow across tube banks.

Chem Eng Proc: Proc Intensification 2000;39:1–14.

[7] Odabaee M, DePaepe M, DeJaeger P, T'Joen C, Hooman K. Particle deposition effects on heat and fluid flow through a metal foam-wrapped tube bundle. *Int J Numer Method Heat Fluid Fl* 2012;23:2–14.

[8] Li T, Deen NG, Kuipers JAM. Numerical study of hydrodynamics and mass transfer of in line fiber arrays in laminar cross-flow. 3rd Int Conf CFD Minerals and Pro Inds CSIRO. Melbourne, Australia; 2003: 87–92.

[9] Yianneskis M, Papadakis G, Balabani S, Castiglia D. An experimental and numerical study of the flow past elliptic cylinder arrays. *Proc Inst Mech Eng C J Mech Eng Sci* 2001;215:1287–301.

[10] Tang LH, Zeng M, Wang QW. Experimental and numerical investigation on air-side performance of fin-and-tube HEs with various fin patterns. *Exp Therm Fluid Sci* 2009;33:818–27.

[11] Mandhani VK, Chhabra RP, Eswaran V. Forced convection heat transfer in tube banks in CF. *Chem Eng Sci* 2002;57:379–91.

[12] Juncu G. A numerical study of momentum and forced convection heat transfer around two tandem circular cylinders at low Reynolds numbers. Part I: Momentum transfer. *Int J Heat Mass Transf* 2007;50:3788–98.

[13] Žukauskas A. Heat transfer from tubes in crossflow. *Adv Heat Transf* 1972;8:93–158.

[14] Khan MG, Fartaj A, Ting DSK. An experimental characterization of cross-flow cooling of air via an in-line elliptical tube array. *Int J Heat Fluid Fl* 2004;25:636–48.

[15] Bravoort MJ, Tifford AN. An experimental investigation of flow across tube banks. USA: NACA; 1942.

[16] Kang HJ, Li W, Li HZ, Xin RC, Tao WQ. Experimental study on heat transfer and PD characteristics of four types of plate fin-and-tube HE surfaces. *J Therm Sci* 1994;3:34–42.

[17] Yao S, Zhu D. Experimental research on heat transfer and PD of two configurations of pin finned-tubes in an in-line array. *J Therm Sci* 1994;3:167–72.

[18] Rahmani R, Mirzaee I, Shirvani H. Computation of a laminar flow and heat transfer of air for staggered tube arrays in cross-flow. *Iran J Mech Eng* 2005;6:19–33.

[19] Marchi CH, Hobmeir MA. Numerical solution of staggered circular tubes in two-dimensional laminar forced convection. *J Braz Soc Mech Sci Eng* 2007;29:42–8.

[20] Jayavel S, Tiwari S. Numerical study of heat transfer and PD for flow past inline and staggered tube bundles. *Int J Numer Meth Heat Fluid Fl* 2009;19:931–49.

[21] Tutar M, Holdo AE. Computational modelling of flow around a circular cylinder in sub-critical flow regime with various turbulence models. *Int J Numer Meth Fl* 2001;35:763–84.

[22] Matos RS, Vargas JVC, Laursen TA, Bejan A. Optimally staggered finned circular and elliptic tubes in forced convection. *Int J Heat Mass Transf* 2004;47:1347–59.

[23] Sumner D. Two circular cylinders in cross-flow: A review. *J Fluid Struct* 2010;26:849–99.

[24] Nishimura T, Itoh H, Ohya K, Miyashita H. Experimental validation of numerical analysis of flow across tube banks for laminar flow. *J Chem Eng Jap* 1991;24:666–9.

[25] Rodgers P, Goharzadeh A, Ali OAE, Eveloy V. An experimental and numerical investigation of tube bank HE thermofluids. 9th Int Conf Therm, Mech multi-physics Sim Exp microelectronics and micro-Syst, EuroSimE2008. 2008.

[26] El-Shaboury AMF, Ormiston SJ. Analysis of laminar forced convection of air crossflow in in-line tube banks with nonsquare arrangements. *Numer Heat Transf. A* 2005;48:99–126.

[27] Jang J-Y, Wu M-C, Chang W-J. Numerical and experimental studies of three

dimensional plate-fin and tube HEs. *Int J Heat Mass Transf* 1996;39:3057–66.

[28] Idem SA, Jacobi AM, Goldschmidt VW. Heat transfer characterization of a finned-tubed HE (with and without condensation). *J Heat Transf* 1990;112: 64–70.

[29] Fowler AJ, Bejan A. Forced convection in banks of inclined cylinders at low Reynolds numbers. *Int J Heat Fluid Fl* 1994;15:90–9.

[30] Murray DB. A comparison of heat transfer in staggered and inline tube banks with a gas-particle crossflow. *Exp Therm Fluid Sci* 1993;6:177–85.

[31] Lu C-W, Huang J-M, Nien WC, Wang C-C. A numerical investigation of the geometric effects on the performance of plate finned-tube HE. *Energ Convers Manage* 2011;52:1638–43.

[32] Rocha LAO, Saboya FEM, Vargas JVC. A comparative study of elliptical and circular sections in one- and two-row tubes and plate fin HEs. *Int J Heat Fluid Fl* 1997;18:247–52.

[33] Saboya FEM, Sparrow EM. Local and average transfer coefficients for one-row plate fin and tube HE configurations. *J Heat Transf* 1974;96:265–72.

[34] Saboya FEM, Sparrow EM. Transfer characteristics of two-row plate fin and tube HE configurations. *Int J Heat Mass Transf* 1976;19:41–9.

[35] Saboya FEM, Sparrow EM. Experiments on a three-row fin and tube HE. *J Heat Transf* 1976;98:520–2.

[36] Kim J-Y, Song T-H. Effect of tube alignment on the heat/mass transfer from a plate fin and two-tube assembly: naphthalene sublimation results. *Int J Heat Mass Transf* 2003;46:3051–9.

[37] Fiebig M, Grosse-Gorgemann A, Chen Y, Mitra NK. Conjugate heat transfer of a finned tube part a: heat transfer behavior and occurrence of heat transfer reversal. *Numer Heat Transf. A* 1995;28:133–46.

[38] Arefmanesh A, Alavi MA. A hybrid finite difference-finite element method for solving the 3D Ee in non-isothermal flow past over a tube. *Int J Numer Meth Heat Fluid Fl* 2008;18:50–66.

[39] Dhaubhadel MN, Reddy JN, Telionis DP. Penalty finite-element analysis of coupled fluid flow and heat transfer for in-line bundle of cylinders in CF. *Int J Non-Linear Mech* 1986;21:361–73.

[40] Fu W-S, Tong B-H. Numerical investigation of heat transfer from a heated oscillating cylinder in a cross flow. *Int J Heat Mass Transf* 2002;45:3033–43.

[41] Chang Y, Beris AN, Michaelides EE. A numerical study of heat and momentum transfer for tube bundles in crossflow. *Int J Numer Meth Fluids*. 1989;9:1381–94.

[42] Tahseen, T.A., M. Ishak, and M. Rahman, Estimation of Heat Transfer and PD in an In-Line Flat Tubes Bundle by Radial Basis Function Network (RBFN).

[43] Tahseen, T.A., M. Rahman, and M. Ishak, Effect of tube spacing, fin density and Reynolds number on overall heat transfer rate for IL configuration. *International Journal of Automotive & Mechanical Engineering*, 2015. 12.

[44] Jassim, A.H., et al., Hybrid CFD-ANN Scheme for Air Flow and Heat Transfer Across IL Flat Tubes Array. *Tikrit Journal of Engineering Sciences*, 2018. 25(2): p. 59-67.

[45] Tahseen, T.A., M. Rahman, and M. Ishak, Heat transfer and PD prediction in an IL flat tube bundle by radial basis function network. *International Journal of Automotive and Mechanical Engineering*, 2014. 10: p. 2003-15.

[46] Shinya A, Terukazu O, Hajime T. Heat transfer of tubes closely spaced in an in-line bank. *Int J Heat Mass Transf.* 1980;23:311–9.

[47] Faghri M, Rao N. Numerical computation of flow and heat transfer in finned and unfinned tube banks. *Int J Heat Mass Transf* 1987;30:363–72.

[48] Krishne Gowda YT, Aswatha Narayana PA, Seetharamu KN. Finite element analysis of

mixed convection over in-line tube bundles. *Int J Heat Mass Transf* 1998;41:1613–9.

[49] Krishne Gowda YT, Patnaik BSVP, Aswatha Narayana PA, Seetharamu KN. Finite element simulation of transient laminar flow and heat transfer past an in-line tube bank. *Int J Heat Fluid Fl* 1998;19:49–55.

[50] Tahseen, T.A., M. Ishak, and M. Rahman. An experimental study of heat transfer and FF characteristics of finned flat tube banks with IL tubes configurations. in *Applied Mechanics and Materials*. 2014. Trans Tech Publ.

[51] Ishak, M., T.A. Tahseen, and M.M. Rahman, Experimental investigation on heat transfer and PD characteristics of air flow over a staggered flat tube bank in crossflow. *International Journal of Automotive and Mechanical Engineering*, 2013. 7: p. 900.

[52] Krishne Gowda YT, Aswatha Narayana PA, Seetharamu KN. Numerical investigation of mixed convection heat transfer past an in-line bundle of cylinders. *Heat Mass Trans* 1996;31:347–52.

[53] Wang M, Georgiadis JG. Conjugate forced convection in crossflow over a cylinder array with volumetric heating. *Int J Heat Mass Transf* 1996;39:1351–61.

[54] Jun Y-D, Tabakoff W. Numerical simulation of a dilute particulate flow (laminar) over tube banks. *J Fluids Eng* 1994;116:770–7.

[55] Mavridou SG, Bouris DG. Numerical evaluation of a HE with inline tubes of different size for reduced fouling rates. *Int J Heat Mass Transf* 2012;55:5185–95.

[56] Aiba S, Ota T, Tsuchida H. Heat transfer of tubes closely spaced in an in-line bank. *Int J Heat Mass Transf* 1980;23:311–9.

[57] Launder BE, Massey TH. The numerical prediction of viscous flow and heat transfer in tube banks. *J Heat Transf* 1978;100:565–71.

[58] Bouris D, Bergeles G. Two dimensional time dependent simulation of the subcritical flow in a staggered tube bundle using a subgrid scale model. *Int J Heat Fluid Fl* 1999;20:105–14.

[59] Roychowdhury DG, Das SK, Sundararajan T. Numerical simulation of laminar flow and heat transfer over banks of staggered cylinders. *Int J Numer Meth Fluids* 2002;39:23–40.

[60] Comini G, Croce G. Numerical simulation of convective heat and mass transfer in banks of tubes. *Int J Numer Meth Eng* 2003;57:1755–73.

[61] Mangadoddy N, Prakash R, Chhabra RP, Eswaran V. Forced convection in CF of power law fluids over a tube bank. *Chem Eng Sci* 2004;59:2213–22.

[62] Liang C, Papadakis G. Large eddy simulation of cross-flow through a staggered tube bundle at subcritical Reynolds number. *J Fluid Struct* 2007;23:1215–30.

[63] Kritikos K, Albanakis C, Missirlis D, Vlahostergios Z, Goulas A, Storm P. Investigation of the thermal efficiency of a staggered elliptic-tube HE for aeroengine applications. *Appl Therm Eng* 2010;30:134–42.

[64] Zhang L-Z, Zhong W-C, Chen J-M, Zhou J-R. Fluid flow and heat transfer in plate-fin and tube HEs in a transitional flow regime. *Numer Heat Transf. A* 2011;60:766–84.

[65] Wang L-C, Su M, Hu W-L, Lin Z-M, Wang L-B, Wang Y. The characteristic temperature in the definition of heat transfer coefficient on the fin side surface in tube bank fin HE. *Numer Heat Transf. Part A* 2011;60:848–66.

[66] Fan JF, Ding WK, He YL, Tao WQ. Three-dimensional numerical study of fluid and heat transfer characteristics of dimpled fin surfaces. *Numer Heat Transf. A* 2012;62:271–94.

[67] Antonopoulos KA. Heat transfer in tube assemblies under conditions of laminar axial, transverse and inclined flow. *Int J Heat Fluid Fl* 1985;6:193–204.

[68] Nishimura T, Kawamura Y. Analysis of flow across tube banks in low Reynolds number region. *J Chem Eng Jap* 1981;14:267–72.

[69] Miyatake O, Iwashita H. Laminar–flow heat transfer to a fluid flowing axially between cylinders with a uniform surface temperature. *Int J Heat Mass Transf* 1990;33:417–25.

[70] Miyatake O, Iwashita H. Laminar–flow heat transfer to a fluid flowing axially between cylinders with a uniform wall heat flux. *Int J Heat Mass Transf* 1991;34:322–7.

[71] Lin C-W, Jang J-Y. 3D Numerical heat transfer and fluid flow analysis in plate–fin and tube HEs with electrohydrodynamic enhancement. *Heat Mass Transf* 2005;41:583–93.

[72] Awad MM, Mostafa HM, Sultan GI, Elbooz A. Performance enhancement of air–cooled condensers. *Acta Polytech Hungarica* 2007;4:125–42.

[73] Şahin HM, Dal AR, Baysal E. 3–D Numerical study on the correlation between variable inclined fin angles and thermal behavior in plate fin–tube HE. *Appl Therm Eng* 2007;27:1806–16.

[74] Taler D. Effect of thermal contact resistance on the heat transfer in plate finned tube HEs. *HE Fouling and Cleaning VII*. 2007;RP5:362–71.

[75] Haider MJ, Danish SN, Khan WA, Mehdi SU, Abbasi BA. Heat transfer and fluid flow over circular cylinders in CF. *NUST J Eng Sci* 2010;3:67–77.

[76] Khudheyer AF, Mahmoud MS. Numerical analysis of fin–tube plate HE by using CFD technique. *ARPN J Eng Appl Sci* 2011;6:1–7.

[77] Cui J, Li WZ, Liu Y, Zhao YS. A new model for predicting performance of fin–and–tube HE under frost condition. *Int J Heat Fluid Fl* 2011;32:249–60.

[78] Perić M, Lenić K, Trp A. A three–dimensional numerical analysis of complete crossflow HEs with conjugate heat transfer. *Eng Rev* 2013;33:23–40.

[79] Li X, Wu X. Thermal mixing of the CF over tube bundles. *Int J Heat Mass Transf* 2013;67:352–61.

[80] Jin Y, Tang G–H, He Y–L, Tao W–Q. Parametric study and field synergy principle analysis of H–type finned tube bank with 10 rows. *Int J Heat Mass Transf* 2013;60:241–51.

[81] Ladjedel O, Adjout L, Yahiaoui T, Imine O. CFD analysis of turbulent cross–flow in a staggered tube bundle equipped with grooved cylinders. *EPJ Web Conf: EDP Sci* 2013.

[82] Shah KN, Patel PD, Mahant KV, Yadav CO. CFD analysis of HE over a staggered tube bank for different angle arrangement of tube bundles. *Int J Eng* 2013;2:1–5.

[83] Karmo D, Ajib S, Khateeb AA. New method for designing an effective finned HE. *Appl Therm Eng* 2013;51:539–50.

[84] Wen J, Tang D, Wang Z, Zhang J, Li Y. Large eddy simulation of flow and heat transfer of the flat finned tube in direct air–cooled condensers. *Appl Therm Eng* 2013;61:75–85.

[85] Li X, Wu X, He S. Numerical investigation of the turbulent CF and heat transfer in a wall bounded tube bundle. *Int J Therm Sci* 2014;75:127–39.

[86] Aslam Bhutta MM, Hayat N, Bashir MH, Khan AR, Ahmad KN, Khan S. CFD applications in various HEs design: A review. *Appl Therm Eng* 2012;32:1–12.

[87] Paul SS, Ormiston SJ, Tachie MF. Experimental and numerical investigation of turbulent cross–flow in a staggered tube bundle. *Int J Heat Fluid Fl* 2008;29:387–414.

[88] Ferziger JH, Perić M. Computational methods for fluid dynamics. 2nd ed. New York: Springer; 1999.

[89] Łopata S, Ocłoń P. Modelling and optimizing operating conditions of HE with finned elliptical tubes. In: Juarez LH, editor. *Fluid Dynamics, Computational Modeling and Applications Europe & China: InTech*; 2012. p. 227–356.

[90] Bhuiyan AA, Islam AKMS, Amin MR. Numerical prediction of laminar characteristics of fluid flow and heat transfer in finned-tube HEs. *Innovative Sys Des Eng* 2011;2:1–12.

[91] Bhuiyan AA, Amin MR, Islam AKMS. Three-dimensional performance analysis of plain fin tube HEs in transitional regime. *Appl Therm Eng* 2013;50:445–54.

[92] Huang C-H, Yuan IC, Ay H. A three-dimensional inverse problem in imaging the local heat transfer coefficients for plate finned-tube HEs. *Int J Heat Mass Transf* 2003;46:3629–38.

[93] Motamedi A, Pacheco-Vega A, Pacheco JR. Numerical analysis of a multi-row multi-column compact HE. 6th Eur Therm Sci Conf (Eurotherm 2012). Poitiers, France: IOP Publishing; 2012.

[94] Bastani A, Fiebig M, Mitra NK. Numerical studies of a compact fin-tube HE. In: Roetzel W, Heggs P, Butterworth D, editors. *Design and operation of HEs*: Springer Berlin Heidelberg; 1992. p. 154–63.

[95] Romero-Méndez R, Sen M, Yang KT, McClain R. Effect of fin spacing on convection in a plate fin and tube HE. *Int J Heat Mass Transf* 2000;43:39–51.

[96] Tutar M, Akkoca A. Numerical analysis of fluid flow and heat transfer characteristics in three-dimensional plate fin-and-tube HEs. *Numer Heat Transf. A* 2004;46:301–21.

[97] Kim YY, Kim KS, Jeong GH, Jeong S. An experimental study on the quantitative interpretation of local convective heat transfer for a plate fin and tube HE using the lumped capacitance method. *Int J Heat Mass Transf* 2006;49:230–9.

[98] Bougeard D. Infrared thermography investigation of local heat transfer in a plate fin and two-tube rows assembly. *Int J Heat Fluid Fl* 2007;28:988–1002.

[99] Paul SS, Tachie MF, Ormiston SJ. Experimental study of turbulent cross-flow in a staggered tube bundle using particle image velocimetry. *Int J Heat Fluid Fl* 2007;28:441–53.

[100] Smith BL, Stepan JJ, McEligot DM. Velocity and pressure measurements along a row of confined cylinders. *J Fluid Eng* 2007;129:1314–27.

[101] Qing-shan Z, Glasenapp T, Ying-zheng L. PIV measurement of fluid flow through staggered tube array. P 13th Asian Congr Fluid Mech Dhaka, Bangladesh; 2010: 1034–8.

[102] Iwaki C, Cheong KH, Monji H, Matsui G. PIV measurement of the vertical cross-flow structure over tube bundles. *Exp Fluid* 2004;37:350–63.

[103] T. A. Tahseen, M. Ishak, and M. M. Rahman, “An overview on thermal and fluid flow characteristics in a plain Fin finned and un-finned tube banks HE,” *Renew. Sustain. Energy Rev.*, vol. 43, pp. 363–380, 2015.

[104] Gianolio E, Cuti F. Heat transfer coefficients and PDs for air coolers with different numbers of rows under induced and forced draft. *Heat Transfer Eng* 1981;3:38–48.

[105] Stasiulevičius J, Skrinska A. *Heat transfer of finned tube bundles in crossflow*. USA: Hemisphere Publishing Corporation; 1988.

[106] Ishigai S, Nishikawa E, Yagi E. Structure of gas flow and vibration in tube banks with tube axes normal to flow. *Int Symposium Mar Eng*, Tokyo; 1973:23–33.

[107] Wung T-S, Chen CJ. Finite analytic solution of convective heat transfer for tube arrays in crossflow: Part 1–Flow field analysis. *J Heat Transf* 1989;111: 633–40.

[108] Achenbach E. Heat transfer from smooth and rough in-line tube banks at high Reynolds number. *Int J Heat Mass Transf* 1991;34:199–207.

[109] Jang J-Y, Yang J-Y. Experimental and 3-D numerical analysis of the thermal-hydraulic characteristics of elliptic finned-tube HEs. *Heat Transfer Eng* 1998;19:55–67.

[110] Ay H, Jang JY, Yeh J-N. Local heat transfer measurements of plate finned-tube HEs

by infrared thermography. *Int J Heat Mass Transf* 2002;45:4069–78.

[111] Tang S, Yang K-T. Thermal performance of a single-row fin-and-tube HE. *J Therm Sci* 2005;14:172–80.

[112] He YL, Tao WQ, Song FQ, Zhang W. Three-dimensional numerical study of heat transfer characteristics of plain plate fin-and-tube HEs from view point of field synergy principle. *Int J Heat Fluid Fl* 2005;26:459–73.

[113] Borrajo-Peláez R, Ortega-Casanova J, Cejudo-López JM. A three-dimensional numerical study and comparison between the air side model and the air/water side model of a plain fin-and-tube HE. *Appl Therm Eng* 2010;30:1608–15.

[114] Paeng JG, Kim KH, Yoon YH. Experimental measurement and numerical computation of the air side convective heat transfer coefficients in a plate fin-tube HE. *J Mech Sci Technol* 2009;23:536–43.

[115] Tang L-H, Min Z, Xie G-N, Wang Q-W. Fin pattern effects on air-side heat transfer and friction characteristics of fin-and-tube HEs with large number of large-diameter tube rows. *Heat Transfer Eng* 2009;30:171–80.

[116] Taler D. Prediction of heat transfer correlations for compact HEs. *Forsch Ingenieurwes* 2005;69:137–50.

[117] Taler D. Determination of heat transfer correlations for plate-fin-and-tube HEs. *Heat Mass Transf* 2004;40:809–22.

[118] Hasan A. Thermal-hydraulic performance of oval tubes in a cross-flow of air. *Heat Mass Transf* 2005;41:724–33.

[119] Hasan A, Sirén K. Performance investigation of plain circular and oval tube evaporatively cooled HEs. *Appl Therm Eng* 2004;24:777–90.

[120] Hasan A, Sirén K. Comparison of external surface heat transfer coefficients for circular and oval tubes. *Heat Transfer Eng* 2007;28:640–4.

[121] Xie G, Sundén B, Wang Q, Tang L. Performance predictions of laminar and turbulent heat transfer and fluid flow of HEs having large tube-diameter and large tube-row by artificial neural networks. *Int J. Heat Mass Transf* 2009;52:2484–97.

[122] Ibrahim TA, Gomaa A. Thermal performance criteria of elliptic tube bundle in crossflow. *Int J Therm Sci* 2009;48:2148–58.

[123] Simo Tala JV, Bougeard D, Russeil S, Harion JL. Tube pattern effect on thermalhydraulic characteristics in a two-rows finned-tube HE. *Int J Therm Sci* 2012;60:225–35.

[124] Robinson KK, Briggs DE. PD of air flowing across triangular pitch banks of finned tubes. *Chem Eng Progr Symposium Ser* 1966;177–84.

[125] Kuntysh VB, Taryan IG, Yakhvedov FM. On the effect of the relative depth of the inter fin space on heat transfer from bundles of finned tubes. *Heat Transfer-Sov Res* 1974;6:5–9.

[126] Rabas TJ, Taborek J. Survey of turbulent forced-convection heat transfer and PD characteristics of low-finned tube banks in CF. *Heat Transfer Eng* 1987;8:49–62.

[127] Rosman EC, Carajilescov P, Saboya FEM. Performance of one- and two-row tube and plate fin HEs. *J Heat Transf* 1984;106:627–32.

[128] Wang C-C, Hsieh Y-C, Lin Y-T. Performance of Plate Finned Tube HEs Under Dehumidifying Conditions. *J Heat Transf* 1997;119:109–17.

[129] Yan W-M, Sheen P-J. Heat transfer and friction characteristics of fin-and-tube HEs. *Int J Heat Mass Transf* 2000;43:1651–9.

[130] Halici F, Taymaz İ, Gündüz M. The effect of the number of tube rows on heat, mass and momentum transfer in flat-plate finned tube HEs. *Energy* 2001;26:963–72.

[131] Kim YH, Kim YC, Kim JR, Sin DS. Effects of fin and tube alignment on the heat transfer performance of finned-tube HEs with large fin pitch. *Int Refrig Air Conditioning Conf. Purdue University*; 2004:1–8.

[132] Khan WA, Culham JR, Yovanovich MM. Convection heat transfer from tube banks in crossflow: Analytical approach. *Int J Heat Mass Transf* 2006;49:4831–8.

[133] Yoo S-Y, Kwonb H-K, Kim J-H. A study on heat transfer characteristics for staggered tube banks in cross-flow. *J Mech Sci Technol* 2007;21:505–12.

[134] Briggs DE, Young EH. Convection heat transfer and PD of air flowing across triangular pitch banks of finned tubes. *Chem Eng Progr symposium Ser* 1963;1:10.

[135] Nir A. Heat transfer and FF correlations for crossflow over staggered finned tube banks. *Heat Transfer Eng.* 1991;12:43–58.

[136] Sparrow EM, Samie F. Heat transfer and PD results for one- and two-row arrays of finned tubes. *Int J Heat Mass Transf* 1985;28:2247–59.

[137] Rabas TJ, Eckels PW, Sabatino RA. The effect of fin density on the heat transfer and PD performance of low-finned tube banks. *Chem Eng Commun* 1981;10:127–47.

[138] Jameson SL. Tube spacing in finned tube banks. *Trans ASME*. 1945;67:633–41.

[139] Fujii M, Fujii T, Nagata T. A numerical analysis of laminar flow and heat transfer of air in an in-line tube bank. *Numer Heat Transf.* 1984;7:89–102.

[140] Antonopoulos KA. Heat transfer in tube banks under conditions of turbulent inclined flow. *Int J Heat Mass Transf* 1985;28:1645–56.

[141] Chen Co-K, Wong K-L, Cleaver JW. Finite element solutions of laminar flow and heat transfer of air in a staggered and an in-line tube bank. *Int J Heat Fluid Fl* 1986;7:291–300.

[142] Wong K-L, Chen C-K. The finite element solutions of laminar flow and combined convection of air in a staggered or an in-line tube-bank. *Wärme- und Stoffübertragung*. 1988;23:93–101.

[143] Chen C-H, Weng F-B. Heat transfer for incompressible and compressible fluid flows over a heated cylinder. *Numer Heat Transf. A* 1990;18:325–42.

[144] Zdravistch F, Fletcher CA, Behnia M. Numerical laminar and turbulent fluid flow and heat transfer predictions in tube banks. *Int J Numer Meth Heat Fluid Fl* 1995;5:717–33.

[145] Cho J, Son C. A numerical study of the fluid flow and heat transfer around a single row of tubes in a channel using immerse boundary method. *J Mech Sci Technol.* 2008;22:1808–20.

[146] Tsai SF, Sheu TWH. Some physical insights into a two-row finned-tube heat transfer. *Comput Fluids* 1998;27:29–46.

[147] Beale SB, Spalding DB. Numerical study of fluid flow and heat transfer in tube banks with stream-wise periodic boundary conditions. *Trans CSME* 1998;22:397–416.

[148] Buyruk E, Johnson MW, Owen I. Numerical and experimental study of flow and heat transfer around a tube in cross-flow at low Reynolds number. *Int J Heat Fluid Fl* 1998;19:223–32.

[149] Buyruk E. Heat transfer and flow structures around circular cylinders in cross-flow. *Turk J Eng Environ Sci* 1999;23:299–315.

[150] Bordalo SN, Saboya FEM. PD coefficients for elliptic and circular sections in one, two and three-row arrangements of plate fin and tube HEs. *J Brazil Soc Mech Sci* 1999;21:600–10.

[151] Wang YQ, Penner LA, Ormiston SJ. Analysis of laminar forced convection of air for crossflow in banks of staggered tubes. *Numer Heat Transf. A* 2000;38:819–45.

[152] Saboya SM, Saboya FEM. Experiments on elliptic sections in one- and two-row arrangements of plate fin and tube HEs. *Experimental Therm Fluid Sci.* 2001;24:67–75.

[153] Li T, Deen NG, Kuipers JAM. Numerical investigation of hydrodynamics and mass transfer for in-line fiber arrays in laminar cross-flow at low Reynolds numbers. *Chem Eng Sci* 2005;60:1837–47.

[154] Khan WA, Culham RJ, Yovanovich MM. Analytical model for convection heat transfer from tube banks. *J Thermophysics Heat Transf* 2006;20:720–7.

[155] Xie G, Wang Q, Sundén B. Parametric study and multiple correlations on air-side heat transfer and friction characteristics of fin-and-tube HEs with large number of large-diameter tube rows. *Appl Therm Eng* 2009;29:1–16.

[156] Tahseen TA, Ishak M, Rahman MM. A numerical study laminar forced convection of air for in-line bundle of cylinders crossflow. *Asian J Sci Res* 2013;6:217–26.

[157] Antonopoulos KA. PD during laminar oblique flow through in-line tube assemblies. *Int J Heat Mass Transf* 1987;30:673–81.

[158] Tahseen TA, Ishak M, Rahman MM. Laminar forced convection heat transfer over staggered circular tube banks: a CFD approach. *J Mech Eng Sci* 2013;4:418–30.

[159] Abdel-Rehim ZS. A numerical study of heat transfer and fluid flow over an in-line tube bank. *Energ Source. A: Recovery, Utilization, and Environmental Effects*. 2012;34:2123–36.

[160] Aiba S, Tsuchida H, Ota T. Heat transfer around tubes in in-line tube banks. *Bulletin of the JSME*. 1982;25: 919–26.

[161] Aiba S, Tsuchida H, Ota T. Heat transfer around tubes in staggered tube banks. *Bulletin of the JSME*. 1982;25:927–33.

[162] Aiba S, Yamazaki Y. An experimental investigation of heat transfer around a tube in a bank. *J Heat Transf* 1976;98:503–8.

[163] Tahseen TA, Ishak M, Rahman MM. A numerical study of forced convection heat transfer for staggered tube banks in cross-flow. 1st Int Conf Mech Eng Res (ICMER), Kuantan, Malaysia; 2011: 216–27.

[164] Ramana PV, Narasimhan A, Chatterjee D. Experimental investigation of the effect of tube-to-tube porous medium interconnectors on the thermohydraulics of confined tube banks. *Heat Transfer Eng* 2010;31:518–26.

[165] Berbish NS. Heat transfer and flow behavior around four staggered elliptic cylinders in CF. *Heat Mass Transf* 2011;47:287–300.

[166] Iacovides H, Launder B, Laurence D, West A. Alternative strategies for modelling flow over in-line tube banks. *Int Symposium on Turbulence and Shear Flow Phenomena (TSFP-8)*. Poitiers, France 2013. p. 1–6.

[167] Jayavel S, Tiwari S. Finite volume algorithm to study the effect of tube separation in flow past channel confined tube banks. *Eng Appl Comput Fluid Mech* 2010;4:39–57.

[168] Lee D, Ahn J, Shin S. Uneven longitudinal pitch effect on tube bank heat transfer in CF. *Appl Therm Eng* 2013;51:937–47.

[169] Kim T. Effect of longitudinal pitch on convective heat transfer in crossflow over in-line tube banks. *Ann Nucl Energ* 2013;57:209–15.

[170] Bejan A, Morega AM. Optimal arrays of pin fins and plate fins in laminar forced convection. *J Heat Transf* 1993;115:75–81.

[171] Cheng YP, Qu ZG, Tao WQ, He YL. Numerical design of efficient slotted fin surface based on the field synergy principle. *Numer Heat Transf. A* 2004;45:517–38.

[172] Rich DG. The effect of fin spacing on the heat transfer and friction performance of multi-row, smooth plate fin-and-tube HEs. *ASHRAE Trans*. 1973;79:137–45.

[173] Webb RL, Kim N-H. *Principle of enhanced heat transfer*. 2nd ed. New York: Taylor & Francis; 2005.

[174] Rich DG. The effect of the number of tube rows on heat transfer performance of smooth plate fin-and-tube HEs. *ASHRAE Trans*. 1975;81:307–17.

[175] McQuiston FC. Correlation of heat, mass and momentum transport coefficients for plate-fin-tube heat transfer surfaces with staggered tubes. *ASHRAE Trans*. 1978;84:294–309.

[176] McQuiston FC. Heat, mass and momentum transfer data for five plate-fin-tube heat transfer surfaces. *ASHRAE Trans*. 1978;84:266–93.

[177] Seshimo Y, Fujii M. An experimental study of the performance of plate fin and tube HEs at low Reynolds number. In: P 3rd

ASME/JSME Therm Eng Joint Conf 1991. p. 449–54.

[178] Kayansayan N. Heat transfer characterization of plate fin–tube HEs. *Heat Recov Syst CHP*. 1993;13:67–77.

[179] Kayansayan N. Heat transfer characterization of flat plain fins and round tube HEs. *Exp Therm Fluid Sci* 1993;6:263–72.

[180] Kayansayan N. Heat transfer characterization of plate fin–tube HEs. *Int J Refrig* 1994;17:49–57.

[181] Wang C-C, Chang Y-J, Hsieh Y-C, Lin Y-T. Sensible heat and friction characteristics of plate fin-and-tube HEs having plane fins. *Int J Refrig* 1996;19:223–30.

[182] Abu Madi M, Johns RA, Heikal MR. Performance characteristics correlation for round tube and plate finned HEs. *Int J Refrig* 1998;21:507–17.

[183] Wang C-C, Chi K-Y. Heat transfer and friction characteristics of plain fin-and-tube HEs, part I: new experimental data. *Int J Heat Mass Transf* 2000;43:2681–91.

[184] Ward DJ, Young EH. Heat transfer and PD of air in forced convection across triangular pitch banks of finned tubes. *Chem Eng Progr Symposium Ser* 1959;55:37–44.

[185] Chen ZQ, Ren JX. Effect of fin spacing on the heat transfer and PD of a two-row plate fin and tube HE. *Int J Refrig* 1988;11:356–60.

[186] Chen Y, Fiebig M, Mitra NK. Conjugate heat transfer of a finned oval tube part B: heat transfer behaviors. *Numer Heat Transf. A* 1998;33:387–401.

[187] Chen Y, Fiebig M, Mitra NK. Conjugate heat transfer of a finned oval tube part A: flow patterns. *Numerical Heat Transf. Part A* 1998;33:371–85.

[188] Sheui TWH, Tsai SF, Chiang TP. Numerical study of heat transfer in two-row HEs having extended fin surfaces. *Numer Heat Transf. A* 1999;35:797–814.

[189] Erek A, Özerdem B, Bilir L, İlken Z. Effect of geometrical parameters on heat transfer and PD characteristics of plate fin and tube HEs. *Appl Therm Eng* 2005;25:2421–31.

[190] Chen H-T, Chou J-C, Wang H-C. Estimation of heat transfer coefficient on the vertical plate fin of finned–tube HEs for various air speeds and fin spacings. *Int J Heat Mass Transf* 2007;50:45–57.

[191] Chen H-T, Lai J-R. Study of heat–transfer characteristics on the fin of two–row plate finned–tube HEs. *Int J Heat Mass Transf* 2012;55:4088–95.

[192] Huang C-H, Yuan IC, Ay H. An experimental study in determining the local heat transfer coefficients for the plate finned–tube HEs. *Int J Heat Mass Transf* 2009;52:4883–93.

[193] Choi JM, Kim Y, Lee M, Kim Y. Air side heat transfer coefficients of discrete plate finned–tube HEs with large fin pitch. *Appl Therm Eng* 2010;30:174–80.

[194] Borrajo–PérezI R, YanagiharaII JI, González–BayónI JJ. Thermal and friction drop characteristic of HEs with elliptical tubes and smooth fins. *Ingeniería Mecánica*. 2012;15:243–53.

[195] Bejan A. Shape and structure, from engineering to nature. New York: Cambridge University Press; 2000.

[196] Bejan A, Sciubba E. The optimal spacing of parallel plates cooled by forced convection. *Int J Heat Mass Transf* 1992;35:3259–64.

[197] Morega AM, Bejan A, Lee SW. Free stream cooling of a stack of parallel plates. *Int J Heat Mass Transf* 1995;38:519–31.

[198] Bejan A, Morega AM. The optimal spacing of a stack of plates cooled by turbulent forced convection. *Int J Heat Mass Transf* 1994;37:1045–8.

[199] Chen H-T, Liou J-T. Optimum dimensions of the continuous plate fin for various tube arrays. *Numer Heat Transf. A* 1998;34:151–67.

[200] Bar–Cohen A, Rohsenow WM. Thermally optimum spacing of vertical, natural

convection cooled, parallel plates. *J Heat Transf* 1984;106:116–23.

[201] Jubran BA, Hamdan MA, Abdualh RM. Enhanced heat transfer, missing pin, and optimization for cylindrical pin fin arrays. *J Heat Transf* 1993;115:576–83.

[202] Bejan A. The optimal spacing for cylinders in crossflow forced convection. *J Heat Transf* 1995;117:767–70.

[203] Stanescu G, Fowler AJ, Bejan A. The optimal spacing of cylinders in free-stream cross-flow forced convection. *Int J Heat Mass Transf* 1996;39:311–7.

[204] Bejan A, Fowler AJ, Stanescu G. The optimal spacing between horizontal cylinders in a fixed volume cooled by natural convection. *Int J Heat Mass Transf* 1995;38:2047–55.

[205] Matos RS, Vargas JVC, Laursen TA, Saboya FEM. Optimization study and heat transfer comparison of staggered circular and elliptic tubes in forced convection. *Int J Heat Mass Transf* 2001;44:3953–61.

[206] Matos RS, Laursen TA, Vargas JVC, Bejan A. Three-dimensional optimization of staggered finned circular and elliptic tubes in forced convection. *Int J Therm Sci* 2004;43:477–87.

[207] Mainardes RLS, Matos RS, Vargas JVC, Ordonez JC. Optimally staggered finned circular and elliptic tubes in turbulent forced convection. *J heat transfer*. 2007;129:674–8.

[208] Canhoto P, Reis AH. Optimization of fluid flow and internal geometric structure of volumes cooled by forced convection in an array of parallel tubes. *Int J Heat Mass Transf* 2011;54:4288–99.

[209] Unuvar A, Kargici S. An approach for the optimum design of HEs. *Int J Energ Res* 2004;28:1379–92.

[210] Hilbert R, Janiga G, Baron R, Thévenin D. Multi-objective shape optimization of a HE using parallel genetic algorithms. *Int J Heat Mass Transf* 2006;49:2567–77.

[211] Saleh K, Abdelaziz O, Aute V, Radermacher R, Azarm S. Approximation assisted optimization of headers for new generation of air-cooled HEs. *Appl Therm Eng* 2012;1–8 [In Press].

[212] Yashar DA, Wojtusiak J, Kaufman K, Domanski PA. A dual-mode evolutionary algorithm for designing optimized refrigerant circuitries for finned-tube HEs. *HVAC&R Res* 2012;18:834–44.

[213] Geb D, Zhou F, DeMoulin G, Catton I. Genetic algorithm optimization of a finned-tube HE modeled with volume-averaging theory. *J Heat Transf* 2013;135:1–10.

[214] Ranut P, Janiga G, Nobile E, Thévenin D. Multi-objective shape optimization of a tube bundle in cross-flow. *Int J Heat Mass Transf* 2014;68:585–98.

[215] Mainardes RLS, Matos RS, Vargas JVC, Ordonez JC. Pumping power minimization in staggered finned circular and elliptic-tube HEs in turbulent flow. *Exp Heat Transf* 2013;26:397–411.

[216] A. Zukauskas. “Heat Transfer from Tubes in CF.” In *Handbook of Single Phase Convective Heat Transfer*, Eds. S. Kakac, R. K. Shah, and Win Aung. New York: Wiley Interscience, 1987.

[217] A. Zukauskas and R. Ulinskas, “Efficiency Parameters for Heat Transfer in Tube Banks.” *Heat Transfer Engineering* no. 2 (1985), pp. 19–25.

[218] Colburn AP. A method of correlating forced convection heat-transfer data and a comparison with fluid friction. (Trans Am I Chem Eng (AIChE), 29; 174–210) reprint by *Int J Heat Mass Transf* 1964;7:1359–84.

[219] Grimison ED. Correlation and utilization of new data on flow resistance and heat transfer for CF of gases over tube banks. *Trans ASME*. 1937;59:583–94.

[220] Kays WM, London AL. *Compact HEs*. New York: McGraw–Hill Ryerson; 1984.

[221] Holman JP. Heat transfer. 10th ed. New York: McGraw–Hill Companies, Inc.; 2010.

[222] Kreith F. Heat and mass Transfer. Mechanical engineering handbook. USA: Boca Raton: CRC Press LLC; 1999.

[223] Incropera FP, Dewitt DP, Bergman TL, Lavine AS. Fundamentals of heat and mass transfer. 6th ed. USA: John Wiley & Sons, Inc; 2011.

[224] Hausen H. Heat transfer in counterflow, parallel flow and CF. New York: McGraw–Hill 1983.

[225] Morgan VT. The overall convective heat transfer from smooth circular cylinders. *Adv Heat Transf.* 1975;11:199–264.

[226] Huge EC. Experimental investigation of effects of equipment size on convection heat transfer and flow resistance in CF of gases over tube banks. *Trans ASME.* 1937;59:573–81.

[227] Pierson OL. Experimental investigation of the influence of tube arrangement on convection heat transfer and flow resistance in CF of gases over tube banks. *Trans ASME.* 1937;59:563–72.

[228] Aiba S. Heat transfer around a tube in in-line tube banks near a plane wall. *J Heat Transf* 1990;112:933–8.

[229] Gray DL, Webb RL. Heat transfer and friction correlations for plate finned–tube HEs having plain fins. In: P 8th Int Heat Transf Conf 1986: 2745–50.

[230] Kim NH, Youn B, Webb RL. Air–side heat transfer and friction correlations for plain fin–and–tube HEs with staggered tube arrangements. *J Heat Transf* 1999;121:662–7.

[231] Wang C–C, Chi K–Y, Chang C–J. Heat transfer and friction characteristics of plain fin–and–tube HEs, part II: Correlation. *Int J Heat Mass Transf* 2000;43:2693–700.

[232] Jakob M. Heat transfer and flow resistance in CF of gases over tube banks. *Trans ASME.* 1938;60:384–6.

[233] Zhang L–Z, Li Z–X. Convective mass transfer and PD correlations for cross–flow structured hollow fiber membrane bundles under low Reynolds numbers but with turbulent flow behaviors. *J Membrane Sci.* 2013;434:65–73.

[234] Wang C–C. Recent progress on the air–side performance of fin–and–tube HEs. *Int J HEs.* 2000;2:57–84.

[235] Tahseen, T.A., M. Rahman, and M. Ishak, *Experimental study on heat transfer and FF in laminar forced convection over flat tube in channel flow.* Procedia Engineering, 2015. **105**: p. 46-55.

[236] Taler D. Experimental determination of correlations for average heat transfer coefficients in HEs on both fluid sides. *Heat Mass Transf* 2013;49:1125–39.

[237] Dittus FW, Boelter LMK. Heat transfer in automobile radiators of the tubular type. University of California, Berkeley, Publications on Eng 2(13): 443–461; reprinted by Int Commun Heat Mass Transf 1985;12:3–22.

[238] Merker GP, Hanke H. Heat transfer and PD on the shell–side of tube–banks having oval–shaped tubes. *Int J Heat Mass Transf* 1986;29:1903–9.

[239] Chen CJ, Wung T–S. Finite analytic solution of convective heat transfer for tube arrays in crossflow: Part II – Heat transfer analysis. *J Heat Transf* 1989;111: 641–8.

[240] Wang C–C, Lee W–S, Sheu W–J. Airside performance of staggered tube bundle having shallow tube rows. *Chem Eng Commun* 2001;187:129–47.

[241] Kim Y, Kim Y. Heat transfer characteristics of flat plate finned–tube HEs with large fin pitch. *Int J Refrig* 2005;28:851–8.

[242] Khan MG, Fartaj A, Ting DSK. Study of cross–flow cooling and heating of air via an elliptical tube array. *ASHRAE Trans* 2005;111:423–33.

[243] Jacimovic BM, Genic SB, Latinovic BR. Research on the air PD in plate finned tube HEs. *Int J Refrig* 2006;29:1138–43.

[244] Min JC, Webb RL. Numerical analyses of effects of tube shape on performance of a finned tube HE. *J Enhanc Heat Transf* 2004;11:63–76.

[245] Bahaidarah HMS. A numerical study of heat and momentum transfer over a bank of flat tubes. Ph.D. Thesis. Texas A&M University; 2004.

[246] Bahaidarah HMS, Anand NK, Chen HC. A numerical study of fluid flow and heat transfer over a bank of flat tubes. *Numer Heat Transf. A* 2005;48:359–85.

[247] Benarji N, Balaji C, Venkateshan SP. Unsteady fluid flow and heat transfer over a bank of flat tubes. *Heat Mass Transf* 2008;44:445–61.

[248] Fullerton TL, Anand NK. Periodically fully-developed flow and heat transfer over flat and oval tubes using a control volume finite-element method. *Numer Heat Transf. A* 2010;57:642–65.

[249] Tahseen AT, Ishak M, Rahman MM. Analysis of laminar forced convection of air for crossflow over two staggered flat tubes. *Int J Automot Mech Eng* 2012;6:753–65.

[250] Tahseen TA, Ishak M, Rahman MM. Performance predictions of laminar heat transfer and PD in an in-line flat tube bundle using an adaptive neuro-fuzzy inference system (ANFIS) model. *Int Commun Heat Mass Transf* 2013; [In Press].

[251] Webb RL, Iyengar A. Oval finned tube conder and design pressure limits. *J Enhanc Heat Transf* 2001;8:147–58.

[252] Ishak M, Tahseen TA, Rahman MM. Experimental investigation on heat transfer and PD characteristics of air flow over a staggered flat tube bank in crossflow. *Int J Automot Mech Eng* 2013;900–11.

[253] Tahseen TA, Ishak M, Rahman MM. An experimental study air flow and heat transfer of air over in-line flat tube bank. 2nd Int Conf Mech Eng Res (ICMER2013). Kuantan, Pahang, Malaysia; 2013.

[254] Horvat A, Mavko B. Drag coefficient and Stanton number behavior in fluid flow across a bundle of wing-shaped tubes. *J Heat Transf* 2006;128:969–73.

[255] Horvat A, Leskovar M, Mavko B. Comparison of heat transfer conditions in tube bundle cross-flow for different tube shapes. *Int J Heat Mass Transf* 2006;49:1027–38.

[256] Horvat A, Mavko B. Heat transfer conditions in flow across a bundle of cylindrical and ellipsoidal tubes. *Numer Heat Transf. A* 2006;49:699–715.

[257] Wang Y, Wang L-C, Lin Z-M, Yao Y-H, Wang L-B. The condition requiring conjugate numerical method in study of heat transfer characteristics of tube bank fin HE. *Int J Heat Mass Transf* 2012;55:2353–64.

[258] Jassim, A.H., et al., An experimental investigation in forced convective heat transfer and FF of air flow over aligned round and flattened tube banks. *Heat Transfer—Asian Research*, 2019. 48(6): p. 2350-2369.

[259] Kundu D, Haji-Sheikh A, Lou DYS. heat transfer predictions in CF over cylinders between two parallel plates. *Numer Heat Transf. A* 1991;19:361–77.

[260] Kundu D, Haji-Sheikh A, Lou DYS. Pressure and heat transfer in CF over cylinders between two parallel plates. *Numer Heat Transf. A* 1991;19:345–60.

[261] Kundu D, Haji-Sheikh A, Lou DYS. Heat transfer in crossflow over cylinders between two parallel plates. *J Heat Transf* 1992;114:558–64.

[262] Bahaidarah HMS, Ijaz M, Anand NK. Numerical study of fluid flow and heat transfer over a series of in-line noncircular tubes confined in a parallel-plate channel. *Numer Heat Transf. B* 2006;50:97–119.

[263] Tahseen AT, Ishak M, Rahman MM. A numerical study of forced convection heat transfer over a series of flat tubes between parallel plates. *J Mech Eng Sci* 2012;3:271–80.

[264] Jue T-C, Wu H-W, Huang S-Y. Heat transfer predictions around three heated cylinders between two parallel plates. *Numer Heat Transf. A* 2001;40:715–33.

[265] Noor Y. A. "constructal design of multi-scale finned tubes cooled by forced convection"

PH.DThesis College of Engineering of Al-Nahrain University 1 2022

[266] T. Bello-Ochende and A. Bejan, "Optimal spacings for mixed convection," *J. Heat Transf.*, vol. 126, no. 6, pp. 956–962, 2004.

[267] M. Joucavel, L. Gosselin, and T. Bello-Ochende, "Maximum heat transfer density with rotating cylinders aligned in cross-flow," *Int. Commun. heat mass Transf.*, vol. 35, no. 5, pp. 557–564, 2008.

[268] E. D. Dos Santos, A. Dallagnol, A. P. Petry, and L. A. O. Rocha, "Heat transfer optimization of cross-flow over assemblies of bluff bodies employing constructal principle," 2009.

[269] L. G. Page, T. Bello-Ochende, and J. P. Meyer, "Maximum heat transfer density rate enhancement from cylinders rotating in natural convection," *Int. Commun. heat mass Transf.*, vol. 38, no. 10, pp. 1354–1359, 2011.

[270] G. Xie, Y. Song, M. Asadi, and G. Lorenzini, "Optimization of pin-fins for a HE by entropy generation minimization and constructal law," *J. Heat Transfer*, vol. 137, no. 6, 2015.

[271] G. Lorenzini, B. S. Machado, L. A. Isoldi, E. D. Dos Santos, and L. A. O. Rocha, "Constructal design of rectangular fin intruded into mixed convective lid-driven cavity flows," *J. Heat Transfer*, vol. 138, no. 10, 2016.

[272] L. Chen, A. Yang, Z. Xie, and F. Sun, "Constructal entropy generation rate minimization for cylindrical pin-fin heat sinks," *Int. J. Therm. Sci.*, vol. 111, pp. 168–174, 2017.

[273] G. M. Barros, G. Lorenzini, L. A. Isoldi, L. A. O. Rocha, and E. D. Dos Santos, "Influence of mixed convection laminar flows on the geometrical evaluation of a triangular arrangement of circular cylinders," *Int. J. Heat Mass Transf.*, vol. 114, pp. 1188–1200, 2017.

[274] A. W. Mustafa, K. H. Suffer, and A. B. Filaih, "Constructal design of flat tubes cooled by natural convection," *Heat Transf.*

[275] A. L. Razera, R. J. C. da Foca, L. A. Isoldi, E. D. dos Santos, L. A. O. Rocha, and C. Biserni, "Constructal design of a semi-elliptical fin intruded in a lid-driven square cavity with mixed convection," *Int. J. Heat Mass Transf.*, vol. 126, pp. 81–94, 2018.

[276] A. Waheed, A. Adil, and A. Razzaq, "The optimal spacing between diamond-shaped tubes cooled by free convection using constructal theory," *Proc. Rom. Acad. Ser. A-MATHEMATICS Phys. Tech. Sci. Inf. Sci.*, vol. 19, pp. 129–134, 2018.

[277] A. W. Mustafa, "Maximization of heat transfer density rate from a single row of rhombic tubes cooled by forced convection based on constructal design," *Heat Transf. Res.*, vol. 48, no. 2, pp. 624–643, 2019.

[278] A. W. Mustafa and I. A. Ghani, "Maximization of heat transfer density from a vertical array of flat tubes in CF under fixed PD using constructal design," *Heat Transf. Res.*, vol. 48, no. 8, pp. 3489–3507, 2019.

[279] A. L. Razera et al., "Fluid flow and heat transfer maximization of elliptic cross-section tubes exposed to forced convection: A numerical approach motivated by Bejan's theory," *Int. Commun. Heat Mass Transf.*, vol. 109, p. 104366, 2019.

[280] A. Bejan and Y. Fautrelle, "Constructal multi-scale structure for maximal heat transfer density," *Acta Mech.*, vol. 163, no. 1, pp. 39–49, 2003.

[281] T. Bello-Ochende and A. Bejan, "Maximal heat transfer density: Fins with multiple lengths in forced convection," *Int. J. Therm. Sci.*, vol. 43, no. 12, pp. 1181–1186, 2004.

[282] T. Bello-Ochende and A. Bejan, "Constructal multi-scale cylinders in cross-flow," *Int. J. Heat Mass Transf.*, vol. 48, no. 7, pp. 1373–1383, 2005.

[283] A. K. Da Silva and A. Bejan, "Constructal multi-scale structure for maximal heat transfer density in natural convection," *Int. J. heat fluid flow*, vol. 26, no. 1, pp. 34–44, 2005.

[284] T. Bello-Ochende and A. Bejan, "Constructal multi-scale cylinders with natural

convection,” *Int. J. Heat Mass Transf.*, vol. 48, no. 21–22, pp. 4300–4306, 2005.

[285] T. Bello-Ochende, J. P. Meyer, and J. Dirker, “Three-dimensional multi-scale Fin assembly for maximum heat transfer rate density,” *Int. J. Heat Mass Transf.*, vol. 53, no. 4, pp. 586–593, 2010.

[286] T. Bello-Ochende, J. P. Meyer, and A. Bejan, “Constructal multi-scale pin–fins,” *Int. J. Heat Mass Transf.*, vol. 53, no. 13–14, pp. 2773–2779, 2010.

[287] Y. Kim, S. Lorente, and A. Bejan, “Constructal multi-tube configuration for natural and forced convection in cross-flow,” *Int. J. Heat Mass Transf.*, vol. 53, no. 23–24, pp. 5121–5128, 2010.

[288] T. Bello-Ochende, J. P. Meyer, and O. I. Ogunronbi, “Constructal multiscale cylinders rotating in cross-flow,” *Int. J. Heat Mass Transf.*, vol. 54, no. 11–12, pp. 2568–2577, 2011.

[289] H. Kobayashi, S. Lorente, R. Anderson, and A. Bejan, “Freely morphing tree structures in a conducting body,” *Int. J. Heat Mass Transf.*, vol. 55, no. 17–18, pp. 4744–4753, 2012.

[290] H. Matsushima, A. Almerbati, and A. Bejan, “Evolutionary design of conducting layers with fins and freedom,” *Int. J. Heat Mass Transf.*, vol. 126, pp. 926–934, 2018.

[291] L. G. Page, T. Bello-Ochende, and J. P. Meyer, “Constructal multi scale cylinders with rotation cooled by natural convection,” *Int. J. Heat Mass Transf.*, vol. 57, no. 1, pp. 345–355, 2013.

[292] A. W. Mustafa, “Constructal design of multi-scale diamond-shaped pin fins cooled by mixed convection,” *Int. J. Therm. Sci.*, vol. 145, p. 106018, 2019.

[293] A. Waheed Mustafa and H. Hussein Abdul Elqadir, “Constructal design of multiscale elliptic tubes in crossflow,” *Heat Transf.*, vol. 49, no. 4, pp. 2059–2079, 2020.

[294] S. C. Haldar, G. S. Kochhar, K. Manohar, and R. K. Sahoo, “Numerical study of laminar free convection about a horizontal cylinder with longitudinal fins of finite thickness,” *Int. J. Therm. Sci.*, vol. 46, no. 7, pp. 692–698, 2007.

[295] E. Ibrahim and M. Moawed, “Forced convection and entropy generation from elliptic tubes with longitudinal fins,” *Energy Convers. Manag.*, vol. 50, no. 8, pp. 1946–1954, 2009.

[296] S. C. Haldar, “Laminar free convection around a horizontal cylinder with external longitudinal fins,” *Heat Transf. Eng.*, vol. 25, no. 6, pp. 45–53, 2004.

[297] J. M. Wu and W. Q. Tao, “Numerical computation of laminar natural convection heat transfer around a horizontal compound tube with external longitudinal fins,” *Heat Transf. Eng.*, vol. 28, no. 2, pp. 93–102, 2007.

[298] C. K. Mangrulkar, A. S. Dhoble, S. G. Chakrabarty, and U. S. Wankhede, “Experimental and CFD prediction of heat transfer and FF characteristics in CF tube bank with integral splitter Fin,” *Int. J. Heat Mass Transf.*, vol. 104, pp. 964–978, 2017.

[299] C. K. Mangrulkar, A. S. Dhoble, S. Chamoli, A. Gupta, and V. B. Gawande, “Recent advancement in heat transfer and fluid flow characteristics in CF HEs,” *Renew. Sustain. Energy Rev.*, vol. 113, p. 109220, 2019.